arXiv:astro-ph/9602130v1 23 Feb 1996

IASSNS-HEP-96/16

On The Rotation And Magnetic Field Evolution Of Superconducting Strange Stars

H. F. Chau[1]
School of Natural Sciences, Institute for Advanced Study, Olden Lane, Princeton, NJ 08540

ABSTRACT

Is pulsar make up of strange matter? The magnetic field decay of a pulsar may be able to give us an answer. Since Cooper pairing of quarks occurs inside a sufficiently cold strange star, the strange stellar core is superconducting. In order to compensate the effect of rotation, different superconducting species inside a rotating strange star try to set up different values of London fields. Thus, we have a frustrated system. Using Ginzburg-Landau formalism, I solved the problem of rotating a superconducting strange star: Instead of setting up a global London field, vortex bundles carrying localized magnetic fields are formed. Moreover, the number density of vortex bundles is directly proportional to the angular speed of the star. Since it is energetically favorable for the vortex bundles to pin to magnetic flux tubes, the rotational dynamics and magnetic evolution of a strange star are coupled together, leading to the magnetic flux expulsion as the star slows down. I investigate this effect numerically and find that the characteristic field decay time is much less than 20 Myr in all reasonable parameter region. On the other hand, the characteristic magnetic field decay time for pulsars is ≥ 20 Myr. Thus, my finding cast doubt on the hypothesis that pulsars are strange stars.

Subject headings: dense matter — magnetic fields — stars: interiors — stars: magnetic fields — stars: rotation

PACS numbers: 97.60.Sm, 12.38.-t, 21.65.+f, 74.20.Ge

[1]e-mail: chau@sns.ias.edu

1. Introduction

What is the most stable form of baryonic matter at high density? This question is of both observational and theoretical interests. With the discovery of pulsars and their identification with the neutron stars in the late 60s, many people thought that neutron star matter is the most stable form of cold condensed matter at high density. This believe was later challenged by Witten. He proposed that at sufficiently high density, deconfinement of nucleons occurs. Moreover, some of the d and u quarks on of the Fermi surface is converted to strange quarks via weak interaction. Thus, the most stable form of matter at ultra-high density is a degenerate mixture of u, d, and s quarks together with a small amount of electrons so as to maintain overall charge neutrality (Witten 1984). This kind of material state is called strange matter. His idea was examined in detail later by Farhi and Jaffe (1984).

The possibility of self gravitating strange matter, namely, a strange star, has also been investigated. The equation of state (EOS) calculations of strange star suggests that they are indeed stable objects in certain parameter range (Alcock et al. 1986; Haensel et al. 1986; Benvenuto and Horvath 1989; see also Madsen and Haensel 1991; and Benvenuto et al. 1991b). The mass and radius of a stable strange star are found to be similar to those of a neutron star. Consequently, some authors suggested that pulsars are in fact strange stars (see for example Benvenuto et al. 1991b). In principle, the question of whether pulsars are neutron or strange stars can be answered by comparing the core density of a neutron star to the strange matter transition density. Unfortunately, all the nuclear physics calculations to date do not yield a definitive answer.

There are a number of difficulties in explaining some of the observational properties of pulsars using the strange star model. The first, and perhaps the most serious difficulty, is the possibility of a strange star glitch. Early EOS calculations suggested that strange stars have very thin nuclear matter crust. The ratio of inertial moment of the nuclear matter crust to that of the whole strange star is of the order of 10^{-5}. Moreover, the density of the nuclear matter crust is not high enough for neutron drip (Alcock et al. 1986; Alcock 1991). In contrast, pulsar glitch observations tell us that the ratio of inertial moment of pinned neutron superfluid crust to that of the whole star is about 10^{-2} (Alpar 1987; Link et al. 1992; Alpar et al. 1993). Nevertheless, by taking into account the existence of strange matter bound states, Benvenuto et al. (1991ab) showed that strange star may support a "strange matter crust" thick enough to account for the observed pulsar glitches. Besides, a more recent calculation suggested that a strange star may be able to retain a reasonable size of nuclear matter crust by accretion as well (Benvenuto et al. 1994).

The second difficulty is the possibility of type I X-ray bursts on a strange star surface. It

is commonly believed that type I X-ray burst involves sudden thermo-nuclear runaway at the surface of an accreting neutron star (see for example Lewin et al. 1993). The same bursting behavior cannot occur on a bare strange star surface because nuclear fuel will dissociate into constituent quarks immediately (Jones 1986). The possibility of X-ray burst,therefore, requires the existence of a nuclear matter crust over a strange star. EOS calculations showed that the nuclear matter crust is separated from the interior strange matter by a electrostatic gap of a few fermi thick, thereby preventing the nuclear matter from converting into strange matter (Alcock et al. 1986; Benvenuto et al. 1991a). A strange pulsar magnetosphere can also be formed, giving rise to the observed radio pulsation (Alcock et al. 1986; Benvenuto et al. 1991b).

The final difficulty is the magnetic field decay time. Assuming a *normal* strange matter core, Jones (1988) pointed that magnetic field inside a strange star will not decay in Hubble's time. Moreover, there is no obvious mechanism for the star to retain a small residual field after say 10^9 years. Therefore, it is inconsistent with both the pulsar magnetic field decay hypothesis, and the spun-up formation scenario of milli-second pulsars (Jones 1988). Nevertheless, the statistical evidence for pulsar magnetic field decay over a period of some 10^9 yr is still inconclusive. Also, milli-second pulsars may rather form by accretion induced collapse of white dwarfs (see for example Bhattacharya and Van den Heuvel 1991 and Bhattacharya and Srinivasan 1995 for discussions on neutron star magnetic field decay). Therefore, the objection of Jones may not be completely well founded. Moreover, as I shall discuss in §2, the core of a strange star is likely to be superconducting. In this case, the magnetic field decay time estimated by Jones (1988) has to be modified. The question of magnetic field decay have been brought up in the review paper by Bailin and Love (1984). They briefly mentioned that the low electron density in the strange stellar core may lead to rapid flux expulsion. However, they did not provide a detail calculation. A major objective of this paper, therefore, is to perform such a calculation, taking into account the coupling between magnetic evolution and rotational dynamics of the star in the presence of collective effects such as clumping of flux tubes.

At this moment, one has no doubt that the standard neutron star model for pulsars is well tested by numerous observational data. However, we still have to keep a close look at the alternative hypothesis, namely, the strange pulsar model (Benvenuto et al. 1991b). In particular, we like to explore various physical properties of a neutron star and a strange star, and to see if there are further ways to test if which of the two models is a better candidate in explaining pulsar observations.

As I shall discuss in §2, the core of a strange star is likely to be superconducting (Bailin and Love 1982, 1984). However, this cast a problem on the rotation of a strange star. In

order to rotate an object with one superconducting species, a uniform magnetic field

$$\mathbf{B} = \frac{2m^*c}{q^*}\,\mathbf{\Omega}\ , \tag{1}$$

called the London field, is set up in the object (Baym 1988), where m^* and q^* are the effective mass and charge of the Cooper pair, and Ω is the rotational angular velocity of the object. But for a strange star, u, d, and s quarks are all superconducting. These superconducting species require different values of B to set up a rotation. Thus, we have a *frustrated* system. The situation is further complicated by the fact that all three superconducting quark flavors interact strongly with each other. In §3, I tackle this rotation problem using Ginzburg-Landau formalism. Instead of setting up a uniform London field, I find that vortices and localized magnetic fields are created when the superconducting quarks rotate together. Then in §4, I point out that the vortices will inter-pin with the magnetic flux tubes, which alter the magnetic field evolution and rotation of a strange star dramatically. In particular, it suggests that the (superconducting) strange pulsar hypothesis is inconsistent with the observed magnetic field decay time in pulsars. Finally, a conclusion is drawn in §5.

2. Strange Matter Superconductivity

Using a relativistic treatment of the BCS theory, Bailin and Love (1982, 1984) suggested that strange matter turns superconducting at low temperatures. Using perturbative QCD at the one gluon exchange level, they showed that the pairing of quarks is most likely to occur in both the ud-du and the ss channels. The ss pairing is expected to have a gap matrix transforming as a color $\underline{\overline{3}}$ and having $J^P = 1^+$ (and hence the pairing is in p-wave). On the other hand, pairing in the u-d system is expected to occur in the isoscalar channel, with a gap matrix transforming as a color $\underline{\overline{3}}$ and having $J^P = 0^+$ (and hence the pairing is in s-wave) (Bailin and Love 1984). The superconducting transition temperature is about 400 keV. Incidentally, the transition temperatures for neutron superfluid and proton superconductor in a neutron star core are of the same order of magnitude. Thus, about 1000 yr after its supernova birth, the interior of a typical strange star is already cold enough for quark superconductivity (Benvenuto and Vucetich 1991). However, one should notice that the above estimation depends quite sensitively on the quark-gluon coupling, and may also change if one goes beyond the one gluon exchange calculations. Thus, the existence of a superconducting core in a strange star is not completely conclusive even though it is very likely. Nonetheless, I assume the existence of quark superconductivity in a strange star core in this paper.

The quark superconductor is likely to be marginally type I with a zero temperature

critical field B_c about 10^{16} G (Bailin and Love 1984). Incidentally, the lower critical field of proton superconductor at the core of a neutron star is also of this order. The typical magnetic field of a canonical pulsar is about 10^{12} G, so naively one would expect complete flux expulsion from the superconducting strange matter core. However, the huge electrical conductivity of the normal state opposes the motion of the flux, thereby, leading to a long flux expulsion time. In the case of a neutron star core, the flux expulsion time is $\sim 10^8$ years (Baym et al. 1969). This time is shorter for strange stars because of their low electron density and strong quark-quark scattering amplitude. Bailin and Love (1982) predicted that it may be as little as 10^4 yr. However, their estimate did not take into account the possibility of flux clumping, which may greatly increase the flux expulsion time. Moreover, if the flux expulsion rate is so fast, then a Meissner state is formed in an old pulsar. As we shall point out in §4.4, the thin crustal nuclear matter is not strong enough to support the magnetic stress and tension of the expelled field. Therefore, we believe that during the life of a canonical pulsar, a meta-stable state with magnetic field penetrating through the superconducting strange star core has to be formed. We shall return to this point later in §4.

Since the quark superfluid also couples to the color vector gluons, color superconductivity may also be observed. Because of color confinement outside the stellar core, we do not have the color analogue of the ambient 10^{12} G magnetic field (Bailin and Love 1984). Thus, the observational consequences of color superconductivity remains unclear.

3. Rotating Strange Star — Ginzburg-Landau Approach

As I have discussed in §1, London magnetic field is set up when a single species of superconducting sample is rotated (Baym 1988; Leggett 1991). In fact, the presence of London field has been observed in terrestrial superconductors (Cabrera 1987). In §3.1, we re-derive the expression in Eq. (1) using Ginzburg-Landau formalism as a warm up to the multi-superconducting-component situation like that in a strange star. In the derivation, I find that there is a critical angular velocity above which the uniform London field state is not the most energetically stable configuration. This critical angular velocity, as far as I know, has not been investigated in the literature. Unfortunately, such a critical angular velocity is too high to be attained experimentally.

3.1. The Case When There Is Only One Superconducting Species

We assume that the Cooper pairs in the sample are in the s-state. Thus, the order parameter for the only superconducting species Ψ is complex. In case the Cooper pairs are in higher angular momentum state, the order parameter will be a complex matrix (Vollhardt and Wölfle 1990). We, however, shall only stick to the simple s-wave pairing derivation. Similar results also apply to higher angular momentum pairing states although the derivation becomes rather complicated. For a sufficiently small angular velocity Ω and sample size, it is reasonable that the speed of the superfluid is not high at any point and hence a non-relativistic treatment will suffice. In the co-rotating frame, the Ginzburg-Landau energy functional reads as $F = \int f\, dV$ where

$$f = -a|\Psi|^2 + \frac{b}{2}|\Psi|^4 + \frac{1}{2m^*}\left|\left(\frac{\hbar\nabla}{i} + \frac{q^*}{c}\mathbf{A} - m^*\mathbf{\Omega}\times\mathbf{r}\right)\Psi\right|^2 + \frac{1}{8\pi}\left|\nabla\times\mathbf{A}\right|^2 \ . \qquad (2)$$

Here, m^* and q^* are the *effective* mass and charge of the Cooper pairs. Moreover, $a, b > 0$ so that the superconducting state is prefered over the normal state. In general, a, and b are temperature dependent. However, a few hundred years after its supernova birth the cooling timescale for a strange star is much longer than its spin-down timescale. Thus, as far as rotational dynamics of the star is concerned, we may assume that a and b are constants.

We consider the case when there is no external magnetic field. The presence of an external magnetic field may simply create extra fluxoids in the sample, which is not very interesting. There are two ways to minimize the kinetic energy term in Eq. (2). First, we can set up a magnetic field so that the $\mathbf{\Omega}\times\mathbf{r}$ contribution is cancelled by $\mathbf{A}$. Alternatively, we can create normal cores (i.e. line defects in the form of vortices similar to that of a rotating superfluid). However, there are prices to pay for both cases: setting up magnetic field requires magnetic energy; setting up vortex needs both a kinetic energy near the vortex and a nucleation energy for creation of the vortex core. What really happens in the sample, in general, is that a uniform magnetic field together with an array of vortices will be formed when it is rotated. Suppose a uniform magnetic field $\mathbf{B}$ (parallel to $\mathbf{\Omega}$) is set up in the star, then $\mathbf{A} = \mathbf{B}\times\mathbf{r}/2$. Then in order to minimize the kinetic energy term in Eq. (2), vortices (or anti-vortices) have to be formed just like a rotating superfluid (see for example Sauls 1989). Unlike fluxoids, vortices carries circulation but not magnetic field. The number of vortex (or anti-vortex) per unit area required is given by

$$n(B) = \frac{2}{\kappa}\left|\Omega - \frac{q^*}{2m^*c}B\right| \ , \qquad (3)$$

where $\kappa = h/m^*$ is the circulation quantum. Obviously, vortices forms an Abrikosov lattice in the absence of spatial inhomogeneity. The Ginzburg-Landau free energy per unit volume

of the system is, therefore, given by (Sauls 1989; Vollhardt and Wölfle 1990)

$$\frac{F}{V} \approx \frac{B^2}{8\pi} + \left\{ \frac{\kappa^2 \rho_s}{4\pi} \left[\ln\left(\frac{R_c}{\xi}\right) - \frac{3}{4} \right] + \frac{1}{2}\,\pi \xi^2 N(0) \Delta^2 \right\} n(B) \ , \tag{4}$$

where $\rho_s = m\Psi^*\Psi$ is the density of superconducting species, ξ is the coherence length of the vortex, R_c is the upper cutoff length which is of the order of the inter-vortex spacing, Δ is the superconducting gap energy, and $N(0)$ is the density of state for one spin projection on the Fermi surface which is given by

$$N(0) = \left[k^2 \frac{dk}{dE_k} \right]_{k=k_F} \approx \frac{E_F^3}{2\pi^2 \hbar^3 c^3} \tag{5}$$

in the extreme relativistic limit.

Physically, the first term in Eq. (4) is the magnetic energy, and the second term is the kinetic and nucleation energies of the vortices. By minimizing Eq. (4), we find that the magnetic field generated in the star is

$$B = \begin{cases} \dfrac{2m^* c}{q^*}\,\Omega & \text{if } \Omega < \Omega_c \\ \dfrac{q^*}{m^* c \kappa} \left\{ \kappa^2 \rho_s \left[\ln\left(\dfrac{R_c}{\xi}\right) - \dfrac{3}{4} \right] + 2\pi^2 \xi^2 N(0) \Delta^2 \right\} & \text{otherwise} \end{cases} \ , \tag{6}$$

where we have neglected the dependence of $\ln R_c$ on B because it is rather weak. The critical angular velocity Ω_c above which vortices begin to form and the translational symmetry of the system is spontaneously broken can be determined from Eqs. (1) and (6). And it is given by

$$\Omega_c = \frac{q^{*2} \rho_s h}{2 m^{*3} c^2} \ . \tag{7}$$

Since magnetic energy scales quadratically with magnetic field while the energy required to form an array of vortices scales linearly with it, formation of vortices is favored at high rotational rates. For a typical terrestrial superconductor (high or low T_c), the effective charge and mass of the Cooper pairs are given by $q^* = -2e$ and $m^* = 2m_e$ respectively. By putting $\rho_s \sim 10^{-6}\,\mathrm{g\,cm^{-3}}$, we obtain $\Omega_c \sim 6 \times 10^8\,\mathrm{rad\,s^{-1}}$. Similarly, for neutron star matter, $q^* = 2e$, $m^* = 2m_p$, and $\rho_s \sim 2 \times 10^{12}\,\mathrm{g\,cm^{-3}}$, $\Omega_c \sim 2 \times 10^{17}\,\mathrm{rad\,s^{-1}}$. Ω_c for strange star matter is similar to that of a neutron star. These angular velocities, unfortunately, are so high that the sample or the star will break apart well before the formation of vortices. In other words, we can neglect the magnetic energy contribution in the Ginzburg-Landau free energy all the time.

3.2. The Case When There Are Multiple Non-interacting Superconducting Species

Now we examine the case when there are more than one superconducting species. We consider the simple case when they are non-interacting. Thus, the only coupling between them is that they response to the *same* vector potential $\mathbf{A}$. If we label each superconducting species by j, the Ginzburg-Landau free energy density is

$$f = \sum_j \left\{ -a_j|\Psi_j|^2 + \frac{b_j}{2}|\Psi_j|^4 + \frac{1}{2m_j^*}\left|\left(\frac{\hbar\nabla}{i} + \frac{q_j^*}{c}\mathbf{A} - m_j^*\mathbf{\Omega}\times\mathbf{r}\right)\Psi_j\right|^2 \right\} + \frac{1}{8\pi}\left|\nabla\times\mathbf{A}\right|^2 \ . \quad (8)$$

Once again, we expect each superconducting species to form vortices in addition to the generation of a common magnetic field. (Compare with Mendell and Lindblom (1991) for a similar study using hydrodynamics.) As we have shown in §3.1, we can neglect the magnetic energy contribution. As a result, for a uniform magnetic field B, the Ginzburg-Landau free energy per unit volume becomes

$$\frac{F}{V} \approx \sum_j \left\{ \frac{\hbar\rho_{sj}}{m_j^*}\left[\ln\left(\frac{R_{cj}}{\xi_j}\right) - \frac{3}{4}\right] + \frac{m_j^*\xi_j^2}{2\hbar}N_j(0)\Delta_j^2 \right\} \left|\Omega - \frac{q_j^*}{2m_j^*c}B\right| \ . \quad (9)$$

As shown in Fig. 1, for a fix Ω, the free energy density contribution of each superconducting species assumes its minimum value when B equals its London magnetic field. Neglecting the weak dependence of $\ln R_c$ on B, F/V is a continuous and piecewise linear function of B with "vertices" locate at the points where B equals the London magnetic field of any one of its superconducting species. Thus, the actual magnetic field B set up in the sample always equals to a London magnetic field of a particular superconducting species. In other words, at least one superconducting species rotates *without* creating vortices. While other species with a different London field have to create vortices (or anti-vortices) in order to rotate with the same angular velocity. This finding is somewhat unexpected because one would naively think that the value of the magnetic field set up in the sample would be a compromise between different London fields and all superconducting species would form vortices. As the superconducting species do not interact, vortices from each species will form Abrikosov lattices on their own (in the absence of spatial inhomogeneity).

What we can predict if the quarks in strange stars were non-interacting? Since the masses (let it be bare or consitutent) of d and u are about the same, which are both much less than that of s, Eq. (1) tells us that their corresponding London fields satisfy

$$B_s < 0 < B_{ud} \quad (10)$$

when $\Omega > 0$. (An exactly reverse relationship is true when $\Omega < 0$.) Since $\rho_u/m_u^* \approx \rho_d/m_d^* \gg$

ρ_s/m_s^* (Alcock 1991), Eq. (8) tells us that $g_{ud} \gg g_s$ where

$$g_j = \frac{\rho_j |q_j^*|}{2 m_j^{*2} c} \qquad \text{for } j = \text{ud,s.} \tag{11}$$

Combining Eqs. (9), (10) and (11), the slope M of our piecewise linear free energy density curve F/V is given by

$$M = \begin{cases} g_s + g_{ud} > 0 & \text{for } B > B_{ud} \\ g_s - g_{ud} < 0 & \text{for } B_s < B < B_{ud} \\ -g_s - g_{ud} < 0 & \text{for } B < B_s \end{cases} , \tag{12}$$

where we have neglected the small nucleation energy contribution in the above estimate.

Consequently, F/V finds its minimum when $B = B_{ud}$. (Readers can verify that this conclusion is independent of the sign of Ω.) So if different flavor quarks were non-interacting, only s quarks would form vortices upon rotation.

3.3. The Case When There Are Multiple Interacting Superconducting Species

Finally, we consider the (realistic) case when the quarks are interacting. The form of the free energy density must be invariant under global phase changes in any of the order parameters. If we consider terms up to second order in gradients and quartic in order parameters, the most general form of f is given by (compare with Alpar et al. 1984b where they have omitted the quartic self-interaction terms)

$$\begin{aligned} f \;=\; & \frac{1}{8\pi}|\nabla \times \mathbf{A}|^2 + \sum_j \left\{ -a_j |\Psi_j|^2 + \frac{1}{2m_j^*} \left| \mathcal{P}_j \Psi_j \right|^2 \right\} + \frac{1}{2} \sum_{j,k} \Big\{ b_{jk} |\Psi_j|^2 |\Psi_k|^2 + \\ & \mu_{jk} (\mathcal{P}_j \Psi_j^*) \cdot (\mathcal{P}_k \Psi_k) \Psi_k^* \Psi_j + \nu_{jk} (\mathcal{P}_j \Psi_j^*) \cdot (\mathcal{P}_k \Psi_k^*) \Psi_j \Psi_k + \\ & \nu_{jk}^* (\mathcal{P}_j \Psi_j) \cdot (\mathcal{P}_k \Psi_k) \Psi_j^* \Psi_k^* \Big\} , \end{aligned} \tag{13}$$

where b is a real symmetric matrix, μ is an hermitian matrix, and

$$\mathcal{P}_j = \frac{\hbar \nabla}{i} + \frac{q_j^*}{c} \mathbf{A} - m_j^* \mathbf{\Omega} \times \mathbf{r} \tag{14}$$

is the covariant momentum operator in the co-rotating frame for the j-th species. Since the free energy has to be bounded from below, we further require all the eigenvalues of the symmetric matrix b to be positive.

To explicitly show the drag effect of one superconducting species on the other, we write the order parameters Ψ_j as $|\Psi_j|\exp(i\varphi_j)$, where φ_j are the phases of the order parameters. Then, the velocity of the superconducting species j in the rotating frame is given by

$$\mathbf{v}_j = \frac{1}{m_j^*\Psi_j}\mathcal{P}_j\Psi_j \approx \frac{\hbar}{m_j^*}\nabla\varphi_j + \frac{q_j^*}{m_j^* c}\mathbf{A} - \mathbf{\Omega}\times\mathbf{r}\ , \tag{15}$$

where we have neglected the spatial variation of $|\Psi_j|$. From Eqs. (13) and (15), we have

$$f = \frac{1}{8\pi}|\nabla\times\mathbf{A}|^2 - \sum_j a_j|\Psi_j|^2 + \frac{1}{2}\sum_{j,k}\left[b_{jk}|\Psi_j|^2|\Psi_k|^2 + \rho_{jk}\mathbf{v}_j\cdot\mathbf{v}_k\right]\ , \tag{16}$$

where

$$\rho_{jj} = m_j^*|\Psi_j|^2 + \mu_{jj}m_j^{*2}|\Psi_j|^4 + 2\nu_{jj}m_j^{*2}|\Psi_j|^4 \tag{17a}$$

and

$$\rho_{jk} = (\mu_{jk} + 2\nu_{jk})\, m_j^* m_k^*|\Psi_j|^2|\Psi_k|^2 \tag{17b}$$

for $j \neq k$. Thus, once a superconducting species moves, Eq. (16) tells us that in general it is energetically favorable for the other superconducting species to move along with it as well. A similar conclusion can be reached by using three-velocity hydrodynamics (Khalatnikov 1957; Andreev and Bashkin 1976; Vardanyan and Sedrakyan 1981).

At the strange matter density, which is about 5×10^{14} gm cm^{-3}, the "fine structure constant" for strong force α_s is about 0.5 – 0.6 (Benvenuto et al. 1991b) indicating that QCD is the dominant interaction between the quark Cooper pairs. The values of the off-diagonal terms of the matrix ρ, which measure the strength of the drag, can be calculated (in principle) from the QCD interaction Hamiltonian. Although the large value of α_s prevents us from using perturbation theory, we believe that the effective coupling constants μ_{ij} and ν_{ij} in Eq. (13) are at least of order of α_s. Thus, the drag force between different quark flavors are so strong that up to first order approximation, all three quark flavors move at the same velocity except possibly near the superfluid cores. The co-moving approximation greatly simplifies our effort to find the minimum system configuration of a strange star.

In order to minimize the drag energy, all the superconducting species have to share common normal cores. We call such a configuration a *vortex bundle*. The circulation of the j-th superconducting species around a circle of radius r centered at the axis of rotation of the star in the co-rotating frame is given by

$$\begin{aligned} 0 &= \oint \mathbf{v}_j\cdot d\mathbf{l} \\ &= \oint \frac{\hbar}{m_j^*}\nabla\varphi_i d\mathbf{l} + \frac{q_j^*}{m_j^* c}\int \mathbf{B}\cdot d\mathbf{S} - \int \nabla\times(\mathbf{\Omega}\times\mathbf{r})\cdot d\mathbf{S} \\ &= \frac{hN_jL}{m_j^*} + \frac{q_j^*\Phi_v L}{m_j^* c} + \frac{q_j^*\pi r^2 B_g}{m_j^* c} - 2\pi r^2\Omega\ , \end{aligned} \tag{18}$$

where Ω is the angular speed of the strange star seen by an external inertial observer, N_j is the number of vortex quantum per bundle for species j, L is the number of vortex bundles, Φ_v is the magnetic flux in the core of a vortex bundle, and B_g is the global uniform (London) magnetic field in the star. Thus, the vortex bundle density $\mathcal{D}$ is given by

$$\mathcal{D}\left(hN_j + \frac{q_j^*\Phi_v}{c}\right) = 2m_j^*\Omega - \frac{q_j^* B_g}{c} \qquad \text{for all } j. \tag{19}$$

Using the same idea, we can show that the speed of superconducting species j at a small distance r from the core of a vortex bundle as seen in the co-rotating frame is given by

$$v_j(r) = \frac{1}{2\pi m_j^* r}\left[hN_j + \frac{q_j^*\Phi_v}{c}\right] + \frac{q_j^* B_g r}{2m_j^* c} - \Omega r \qquad \text{for all } j. \tag{20}$$

Thus, the co-moving requirement of super-currents at all spatial points requires that (a) $q_j^* B_g/2m_j^* c - \Omega$ is a constant for all j, which is possible only if the global uniform London field B_g is zero; and (b) $hN_j/m_j^* + q_j^*\Phi_v/m_j^* c$ is a constant for all j, implying that the integers N_j, and the magnetic flux Φ_v are chosen in such a way that

$$\frac{hN_j}{m_j^*} + \frac{q_j^*\Phi_v}{m_j^* c} = K \tag{21}$$

for some constant $K \neq 0$ for all j. K can be interpreted as the circulation of a vortex bundle in this strongly interacting superconducting system.

The necessary and sufficient conditions for the existence of solution in Eq. (21) are proven in Appendix A. It turns out that the co-moving constraint (Eq. (21)) is very stringent: In general, solution may not exist for a system involving more than two species of superconducting Cooper pairs. And in the case the solution of Eq. (21) does not exist, the only way out is that superconductivity in some species are destroyed. Luckily, in case of the strange star matter, there is only two species of Cooper pairs, namely, ud-du and ss, so that the solution in the strongly interacting limit exists. In this limit, we expect *all* the quark flavors to form quantized vortices when the star rotates. The normal vortex core of each superconducting species shares a common region of space, in the form of vortex bundles. Magnetic field may be present in the vortex bundle cores. Moreover, stellar rotation is made possible by the formation of vortex bundles rather than by a uniform London magnetic field.

In case of the strange star matter, the ud-du and ss Cooper pairs have charges $q_{ud}^* = e/3$ and $q_s^* = -2e/3$, respectively. Also, the effective mass of a strange quark at the strange star interior $m_s \sim 175$ MeV (Benvenuto et al. 1991b). Therefore the effective mass of an ss Cooper pair, m_s^*, is approximately 350 MeV. The effective mass of a u or d quark, m_{ud}, is of

order of 10 MeV, giving $m^*_{ud} \sim 20$ MeV. Since (m_{ud}, q_{ud}) and (m_s, q_s) are linear independent, the solution of Eq. (21) is given by (see Appendix A)

$$\begin{pmatrix} K \\ \Phi_v \end{pmatrix} = \frac{h}{[m^*_s q^*_{ud} - m^*_{ud} q^*_s]} \begin{pmatrix} q^*_{ud} N_s - q^*_s N_{ud} \\ c[m^*_{ud} N_s - m^*_s N_{ud}] \end{pmatrix} , \tag{22}$$

where N_{ud} and N_s are the number of quanta per vortex bundle for ud-du and ss Cooper pairs respectively, and $K \neq 0$. In the zero temperature limit, the system will choose the ground state configuration out of the above infinitely many solutions. Similar to Eq. (4), the Ginzburg-Landau free energy per unit volume in the strongly interacting limit is given by

$$\frac{F}{V} \approx \left\{ \sum_j \left[\frac{h^2 \rho_{sj} N_j^2}{4\pi m_j^{*2}} \left[\ln\left(\frac{R_{cj}}{\xi_j}\right) - \frac{3}{4} \right] + \frac{\pi \xi_j^2}{2} N_j(0) \Delta_j^2 \right] + \frac{\Phi_v^2}{8\pi^2 \lambda^2} \right\} |\mathcal{D}| , \tag{23}$$

where λ is the penetration depth, and $\mathcal{D}$ is the number density of vortex bundles. From Eq. (19), $\mathcal{D}(hN_j + q^*_j \Phi_v/c) = 2m^*_j \Omega$ in the strongly interacting limit. Consequently,

$$\begin{aligned} \frac{F}{V} \approx & \left\{ \sum_j \frac{1}{hN_j c + q^*_j \Phi_v} \left[\frac{h^2 \rho_{sj} N_j^2}{2\pi m^*_j} \left[\ln\left(\frac{R_{cj}}{\xi_j}\right) - \frac{3}{4} \right] + \pi m^*_j \xi_j^2 N_j(0) \Delta_j^2 \right] + \right. \\ & \left. \frac{\Phi_v^2 m^*_1}{4\pi^2 \lambda^2 (hN_1 c + q^*_1 \Phi_v)} \right\} c|\Omega| \end{aligned} \tag{24}$$

increases (approximately) linearly with the angular speed $|\Omega|$ of the star.

Now, we estimate the average free energy density for strange star matter. BCS theory tells us that $\Delta = 1.76 kT_c$ for s-wave paired superconductor. Putting $kT_c \sim 400$ keV for strange stellar matter (Bailin and Love 1984), we find $\Delta_{ud} \sim 700$ keV. The number densities for u and d quarks are given by (Alcock et al. 1986)

$$n_j = \frac{1}{\pi^2} \left(1 - \frac{2\alpha_s}{\pi} \right) \mu_j^3 \qquad \text{for } j = \text{u,d}, \tag{25}$$

where μ_j is the chemical potential. Putting $\alpha_s = 0.5$ and $\mu_u \approx \mu_d \sim 400$ MeV (Benvenuto et al. 1991b), $n_u \approx n_d \sim 5.7 \times 10^{38}$ cm^{-3}. Since the electron number density is much less than that of the quarks (Bailin and Love 1984; Alcock et al. 1986; Benvenuto et al. 1991b), the charge neutrality condition reads

$$\frac{2}{3} n_u - \frac{1}{3} n_d - \frac{1}{3} n_s = n_e \approx 0 . \tag{26}$$

Therefore, we expect $n_s \approx n_d$.

For both u and d quarks, $E_F \approx \mu \sim 400$ MeV (Bailin and Love 1984), and hence from Eq. (5, $N_{ud}(0) \sim 6.6 \times 10^{41}$ erg^{-1} cm^{-3}. Also, $m_u \approx m_d \sim 10$ MeV. The coherence length ξ_j

can be estimated in the framework of relativistic Ginzburg-Landau theory. Bailin and Love (1984) argue that

$$\xi_j^3 \approx \frac{7\zeta(3)}{2kT_{c_j}p_{F_j}\mu_j} \ , \tag{27}$$

where $\zeta(3) \sim 1.20$, and p_{F_j} is the Fermi momentum of species j which is approximately equal to E_{F_j}/c inside a strange star. Thus, $\xi_{ud} \sim 8.0$ fm. Since the quark superconductor is likely to be marginally type I, $\lambda \approx \sqrt{2}\xi_{ud} \sim 11.3$ fm. Assuming $\ln(R_{cj}/\xi_j)$ to be of order of 10, I numerically compute the average free energy density in Eq. (24) for all possible values of N_{ud} and N_s. I find that the ground state configuration for strange star matter is achieved when $N_s = 1$, $N_{ud} = 0$. Consequently, the values of K and Φ_v in the ground state configuration are given by

$$K = \frac{h}{m_s^* - 2m_{ud}^*} \sim 0.012 \text{ cm}^2\,\text{s}^{-1} \tag{28a}$$

and

$$\Phi_v = \frac{3hcm_{ud}^*}{e(m_s^* - 2m_{ud}^*)} \sim 8.0 \times 10^{-8} \text{ G}\,\text{cm}^2 \tag{28b}$$

respectively.

In summary, the star behaves quite differently in the non-interacting and strongly interacting limits. In the non-interacting limit, a global magnetic field is set up, and vortices are formed in all but one superconducting species when the system rotates. In contrast, vortex bundles in the form of Abrikosov lattice is present in a rotating strongly interacting system. Moreover, the global uniform London magnetic field is no longer present. Regarding the coupling between the quarks as a tuning parameter, it is interesting to map out the phase diagram of this system. And this will be carried out in future works.

4. Vortex Inter-pinning And Its Astrophysical Consequences

The formation of vortices in a rotating superconducting strange star has at least three possible observational consequences if one assumes that the observed pulsars are in fact strange stars instead of neutron stars. First, the heat capacity of the star and the cooling processes are modified and its effect on the strange star cooling has been studied (Benvenuto and Vucetich 1991; Page 1992). In this section, we concentrate on the second effect, namely, the magnetic field decay due to inter-pinning of vortex bundles and the magnetic fluxoids. I shall discuss briefly possible magnetic field alignment due to inter-pinning in §4.2 as well.

Nucleation energy is required in the creation of normal cores in both vortex bundles

and magnetic fluxoids in a strange star. Therefore, it is energetically favorable for a vortex bundle to "pin" to a magnetic fluxoid so that a lesser volume of normal strange matter has to be nucleated. Thus, the dynamics of vortex bundles and magnetic flux tubes are coupled together. Similar to the case of superfluid neutron vortices in a rotating neutron star (Alpar et al. 1993), Eq. (24) tells us that in the strongly interacting limit, the quark vortex bundle density is directly proportional to the angular speed $|\Omega|$ of the rotating strange star. As a strange star spins down, its vortex bundles in the star core have to move radially outward from the rotational axis (and eventually some of them will annihilate near the stellar surface). The pinning of quark vortex bundles and magnetic flux tubes implies that the rotational and magnetic evolution of a strange star are coupled.

Alternatively, the vortex bundle and the flux tubes can pin together by interaction of their core magnetic fields. When two magnetic carrying wires are placed together, an energy change of $\mathbf{B}_1 \cdot \mathbf{B}_2 V/4\pi$ is expected, where V is their interacting volume, and $\mathbf{B}_j$ are their magnetic field strength. Depending on their relative field orientation, the two wires experience either mutual attraction or repulsion. In the former case, the wires will pin to each other; and in the latter case, the wires will avoid each other, and hence effectively "pin" to the inter-wire spaces. In fact, similar ideas have been applied to the proton fluxoids and magnetic vortices in neutron star cores; and their possible observational consequences have been studied (Sauls 1989; Srinivasan et al. 1990; Chau et al. 1992; Ding et al. 1993).

4.1. Estimation Of Pinning Energy Per Intersection

Now we estimate the pinning energy per intersection of a vortex bundle with a flux tube by both pinning mechanisms. The pinning energy due to nucleation per intersection is given by

$$(E_p)_{\rm nucl} \approx \frac{1}{2} \sum_j N_j(0) \Delta_j^2 V_j \ . \tag{29}$$

The intersection volume for species j, V_j, is given by

$$V_j \approx \alpha \pi \mathcal{N}_{\rm flux}^{1/2} \xi_j^3 \ , \tag{30}$$

where ξ_j is the coherence length for species j, $\mathcal{N}_{\rm flux}$ is the number of flux quantum in a flux tube, and α is a geometrical factor depending on the angle between the magnetic flux tube and the vortex, θ, and their elastic moduli. For stiff magnetic flux tubes and vortex bundles, $\alpha \approx 2 \, {\rm cosec} \, |\theta|$.

We estimate the nucleation pinning energy as follows: for an s-wave superconductor, BCS theory tells us that $\Delta = 1.76 k T_c$; and for a p-wave superconductor, $\Delta = 2.4 k T_c$ (Baym

and Pethick 1975). Putting $kT_c \sim 400$ keV for strange stellar matter (Bailin and Love 1984), we obtain $\Delta_{ud} \sim 700$ keV and $\Delta_s \sim 960$ keV. For ud-du quark Cooper pairs, $E_F \approx \mu \sim 400$ MeV (Bailin and Love 1984). And beta equilibrium requires $E_{F_s} \approx \mu_s = \mu_d \approx 400$ MeV. The coherence lengths are given by Eq. (27), giving us $\xi_{ud} \approx \xi_s \sim 8$ fm. So from Eqs. (5), (29) and (30), we obtain

$$(E_p)_{\rm nucl} \sim 2.4 \mathcal{N}_{\rm flux}^{1/2} \,{\rm cosec}\,|\theta| \ {\rm MeV}. \tag{31}$$

Similarly, the magnetic pinning energy is given by (Chau et al. 1992; Ding et al. 1993)

$$(E_p)_{\rm mag} \approx \frac{|\mathbf{B}_{\rm vortex} \cdot \mathbf{B}_{\rm fluxoid}|}{4\pi} V \approx \frac{B_c \Phi_v \lambda \mathcal{N}_{\rm flux}^{1/2}}{2\pi} |\cot\theta| \ , \tag{32}$$

where B_c is the critical magnetic field. Since the flux quantum for a strange star flux tube equals $hc/2(2e/3) = 3hc/4e$, and $\lambda \sim 11.3$ fm, we obtain $B_c \sim 7.7 \times 10^{16}$ G. By putting the value of Φ_v obtained in Eq. (28b), we find

$$(E_p)_{\rm mag} \sim 690 \mathcal{N}_{\rm flux}^{1/2} |\cot\theta| \ {\rm MeV}. \tag{33}$$

So, unless the magnetic flux tubes and the vortices are perpendicular to each other (this happens when the rotational and magnetic axes of the star are orthogonal to each other), the magnetic pinning energy is approximately two order of magnitude larger than the nucleation pinning energy. Therefore, we shall use the magnetic pinning energy in our subsequent calculations.

4.2. Forces Acting On Flux Tubes And Vortices

Following Ding et al. (1993), the major forces acting on flux tubes and vortices of a spinning down strange star are summarized below:

(a) *Inter-pinning force:* Since it is energetically favorable for the magnetic flux tubes and the vortex bundles to pin with each other, a force of order of E_p/ξ is experienced by both parties when one tries to pull them apart. (Similar assertion is true when the magnetic pinning force is repulsive.) This inter-pinning force encourages the magnetic flux tubes and vortex bundles to move together.

(b) *Thermal activation:* Since E_p is of order of 100 MeV and the interior temperature of the star is $\lesssim 10$ keV, random thermal noise can be an important source of "force". In particular, thermal activation can depin a vortex with a flux line.

(c) *Magnus force:* The magnetic flux tubes couple to the thin crust of the strange star via electromagnetic interaction between its strong core magnetic field and the background electron plasma. Therefore, the flux tubes co-rotate, and hence spin down, with the crust of the star. The vortex bundle core, due to inter-pinning, may spin down with the crust as well. Eq. (19) tells us that the only way to slow down the angular speed of a rotating superconducting quark fluid is by reducing its vortex bundle density. This can in turn be achieved only by moving the vortex bundles radially outward from the axis of rotation of the star. So as the star slows down, a steady angular velocity difference between the superconducting quark fluid and the crust is developed. Consequently, a hydrodynamic force, called the Magnus force, acting on the vortex bundles is developed. Magnus force tries to push the vortex bundle radially outward from the rotational axis of the star, thereby reducing the angular velocity difference between the superconducting quark fluid and the crust. The combined effect of the Magnus force and the inter-pinning force may cause a spin down induced magnetic field expulsion in a strange star. The Magnus force also defines a preferred direction for the thermal activation (i.e., thermally assisted creeping).

For a inter-winded network of pinned magnetic flux tubes and quark vortex bundles, the average force per unit length acting on a magnetic flux tube due to the Magnus force acting on the vortex bundles is given by (compare with Ding et al. 1993)

$$\mathbf{f}_{f,\mathrm{Mag}} \approx \frac{L_v}{L_f}\,\rho K r\omega\hat{\mathbf{e}}_r \ , \tag{34}$$

where r is the distance from the rotational axis, ω is the angular velocity difference between the superconductor (Ω_s) and the stellar crust (Ω_c), K is the circulation given by Eq. (28a), ρ is the total matter density, L_f and L_v are the total number of flux tubes and vortex bundles respectively in the star. In fact, L_f and L_v can be determined by considering the total magnetic flux and the circulation of superconducting current of the star. They are given by

$$L_f = \frac{4\pi e R_{\mathrm{star}}^2 |B_{\mathrm{star}}|}{3hc\mathcal{N}_{\mathrm{flux}}} \ , \tag{35}$$

and

$$L_v = \frac{2\pi R_{\mathrm{star}}^2 |\Omega|}{K} \equiv \frac{4\pi R_{\mathrm{star}}^2 (m_s - 2m_{ud})}{h}\,|\Omega| \ , \tag{36}$$

where R_{star} and B_{star} are the radius and total magnetic field strength of the star respectively.

The angular velocity difference, ω, is likely to remain at its steady state value, which can be deduced from the vortex creep theory (Alpar et al. 1984a; Alpar et al. 1993) and

is given by

$$\begin{aligned}\omega_\infty &= \pm\frac{kT}{\rho K b_p r\lambda}\sinh^{-1}\left[\frac{r}{4\Omega v_0}|\dot{\Omega}|\exp\left(\frac{E_p}{kT}\right)\right] \\ &\approx \pm\frac{E_p}{\lambda\rho K b_p r} \\ &\approx \pm\frac{B_c\Phi_v|\cos\theta|}{\pi\rho K r}\left(\frac{e|B_{\rm star}|}{3hc}\right)^{1/2} = \pm\omega_{cr}\ ,\end{aligned} \tag{37}$$

where we have assumed that $E_p \gg kT$. Here $v_0 \sim 10^{13}\,{\rm cm\,s^{-1}}$ is the microscopic creeping speed, $b_p \approx (1/|\sin\theta|)\times(\pi R_{\rm star}^2/L_f)^{1/2}$ is the mean distance between successive pinning sites along a vortex bundle, and ω_{cr} is the critical angular velocity lag above which it is no longer energetically favorable for the vortices and fluxoids to pin together. The plus (or minus) sign is taken if the outward moving speed of vortex bundles is greater (or less) than that of magnetic flux tubes. Therefore, the maximum possible average force per unit length vortex bundles can exert on a flux tube equals $\rho K R_{\rm star}\omega_{cr}L_v/L_f$.

Finally, if the spin down of the star is mainly due to its dipole radiation lost, then the outward moving speed of the vortex bundles is given by (Ding et al. 1993)

$$v_v(t) \approx \frac{B_{\rm star}^2 R_{\rm star}^7\Omega^2\sin^2\theta}{3Ic^3}\ , \tag{38}$$

where I is the moment of inertia of the star.

(d) *Buoyancy force:* The presence of magnetic stress in the core of a flux line decreases the internal density of quark matter (Muslimov and Tsygan 1985; Harvey et al. 1986; Jones 1987). Thus, the buoyancy force per unit length experienced by a flux line is

$$\mathbf{f}_{\rm buoy} = \frac{9h^2c^2\mathcal{N}_{\rm flux}g}{128e^2\pi^2\lambda^2c_s^2}\,\hat{\mathbf{e}}_r \approx \frac{9h^2c^2\mathcal{N}_{\rm flux}}{128e^2\pi^2\lambda^2R_{\rm star}}\,\hat{\mathbf{e}}_r\ , \tag{39}$$

where g is the local acceleration due to gravity, $c_s^2 \equiv dP/d\rho \approx gR_{\rm star}$ is the squared sound speed.

(e) *Tension:* The combined pushing of all the vortex bundles pinned onto a given magnetic flux line may globally bend the flux line. In effect, a tension force is developed which tries to resist further deformation. The average tension per unit length is given by (Harvey et al. 1986)

$$\mathbf{f}_{\rm tens} = -\frac{9h^2c^2\mathcal{N}_{\rm flux}}{256e^2\pi^2\lambda^2}\ln\left(\frac{\lambda}{\xi}\right)\frac{1}{s_c}\,\hat{\mathbf{e}}_r \approx -\frac{R_{\rm star}f_{\rm buoy}}{2s_c}\ln\left(\frac{\lambda}{\xi}\right)\,\hat{\mathbf{e}}_r\ , \tag{40}$$

where s_c is the radius of curvature of the flux tube.

(f) *Electron drag force:* As a flux tube drifts out of the core, it will experience a drag force arising from the scattering of the degenerate relativistic electron. This drag force limits the speed of the flux tubes and hence the rate of magnetic field decay. In the absence of clumping of flux tubes, the drag force per unit length is given by[2] (Muslimov and Tsygan 1985; Harvey et al. 1986; Jones 1987)

$$\mathbf{f}_{\rm drag} = -\frac{27\pi}{1024}\,\frac{n_e h^2 c \mathcal{N}_{\rm flux}^{3/2} v_f}{E_f(e)\lambda}\,\hat{\mathbf{e}}_r \ , \tag{41}$$

where $E_f(e)$ is the electron Fermi energy, v_f is the velocity of the flux tube, and n_e is the electron number density and is given by (Alcock et al. 1986)

$$n_e = \frac{\mu_e^3}{3\pi^2} \ . \tag{42}$$

The electron chemical potential in a strange star is about 20 MeV (Benvenuto et al. 1991b), giving us $n_e \sim 3.5 \times 10^{34}$ cm^{-3}. Thus, the electron number density is some two orders of magnitude smaller than that of a neutron star. Consequently, the electron drag force in a strange star is much weaker than that in a neutron star.

The average radial velocity of a flux tube is approximately equal to its steady state radial velocity v_f, which can be calculated from the force balance equation

$$\mathbf{f}_{\rm f,Mag} + \mathbf{f}_{\rm buoy} + \mathbf{f}_{\rm tens} + \mathbf{f}_{\rm drag} = \mathbf{0} \ . \tag{43}$$

After finding v_f, the magnetic field $B_{\rm star}$ of the star can be computed by solving the equation (compare with the $\dot{\Omega}$ equation in Alpar et al. 1984a)

$$\dot{B}_{\rm star} = -\frac{2B_{\rm star} v_f}{R_{\rm star}} \ . \tag{44}$$

4.3. The Alignment Torque

In general, magnetic flux tubes incline at a non-zero angle θ to the rotational axis of the star. Thus, the magnitude (and sometimes even the direction) of force acting on a flux tube by the vortex bundles changes as we go along the flux tube itself. The combined forces acting on a magnetic flux tube due to vortex bundles, therefore, produce a total force together with

[2]Note that there is an extra factor of 9/4 because the flux quantum for proton superconductor and strange matter superconductor are different. In addition, the case of flux clumping will be addressed in §4.5.

a torque (Ruderman 1991abc). While the total force may lead to a magnetic field decay in a spinning down strange star, the torque tends to push the field lines towards the equator as the star spins down. Similarly, it tends to push the field lines towards the poles as the star spins up (Ruderman 1991b).

The effect of this torque on the time evolution of magnetic field is not completely clear. If the crustal material of a strange star, which makes up of nuclear instead of strange matter, is strong enough to support a shear, then the direction of magnetic field will not change with time. On the other hand, if the crustal nuclear material is weak and brittle, direction of magnetic field may change via a series of "crust cracking" (Ruderman 1991abc). A more complete discussion on the effect of this alignment torque will be reported in future works.

4.4. The Crustal Magnetic Field

So far, I am concentrating on the magnetic field in the core of the star. In this subsection, I show that the presence of crustal magnetic field does not seriously affect the magnetic field evolution of a strange star. The density of the strange stellar crust must be below the neutron drip density ($\sim 4.3 \times 10^{11}$ gm cm^{-3}), otherwise the dripped neutrons can convert into strange matter by making contact with them. Since the most favorable nucleus just below neutron drip is ^{118}Kr (Baym and Pethick 1975), spacing between the nuclear lattice just below the neutron drip b is about 70 fm. Hence, the Young's modulus of this lattice is about $(Ze)^2/b^4 \sim 10^{29}$ dyn cm^{-2}. (The Young's modulus of the nuclear lattice is much smaller if it is not prefect or if the density of the crust is lower than for the neutron drip.) If the magnetic flux is completely expelled from the core, the inner layer of the normal matter crust has to sustain a stress of $\approx B^2 \Delta R/4\pi$ per unit length, where $\Delta R \sim 100$ m is the thickness of the crust. The magnetic stress lengthens the nuclear lattice; however, such a lengthening must not be greater than the $\lesssim 10$ fm electro-static gap between strange and nuclear matter in the star. Otherwise, strange matter conversion will take place and the crust will be destroyed. After some computation, I find that the maximum field and flux the nuclear crust can sustain are $\sim 10^7$ G and $\sim 7 \times 10^{17}$ G cm^2 respectively. This is much smaller than the initial magnetic flux of a strange pulsar. So we have two possibilities: (a) there is an efficient field decay mechanism operating in the thin nuclear matter crust; or (2) the crust breaks at some point when majority of the field in the core is expelled, eventually making the star a bare strange matter object. In either case, the contribution of the magnetic field in the crust does not play an important role in the magnetic evolution of the entire star. Thus, we shall neglect the presence of crustal field in our subsequent analysis.

4.5. Magnetic Field Decay — Numerical Results

I numerically compute the magnetic field decay due to inter-pinning of magnetic flux tubes and vortex bundles. I assume that the initial magnetic field $B_{\rm star}(0)$ is uniformly distributed in the stellar core, and we also neglect the existence of a thin nuclear matter crust. The initial angular speed of the star is set to be $\Omega(0)$. The effect of the alignment torque is also ignored. To simplify calculations, we follow Ding et al. (1993) to combine the buoyancy force (Eq. (39)) and the tension force terms (Eq. (40)) because of their similar dependence on parameters. We write

$$f_{\rm buoy} + f_{\rm tens} = \gamma f_{\rm buoy} \ , \tag{45}$$

where $\gamma = 1 - (R_{\rm star}/2s_c)\ln(\lambda/\xi)$ is a time dependent quantity of order of unity in most parts of the star (Harvey et al. 1986).

What happens if the magnetic flux lines form a clump? Provided that the size of such a clump is smaller than the electron mean free path, electrons may collectively scatter with a number of flux lines within a clump leading to a dramatic change in the drag force (Ruderman 1992). In addition, clumping leads to an increase in the local density of pinning centers. Moreover, the force between flux tubes within a clump may be important. Thus, our mean field estimate of the force acting on the flux tubes by the vortex bundles will change as well.

We model the clumping effect by a renormalization scheme. By coarse graining to the level of a clump, the behavior of the flux tubes inside a clump is similar to that of a single magnetic flux tube carrying the same amount of flux as the clump provided that the size of the clump is much smaller than the electron mean free path. In addition, the magnetic field strength in this single magnetic flux tube equals to that in each of the individual flux tubes in the clump. That is, we may replace $\mathcal{N}_{\rm flux}$ by $\mathcal{N}_{\rm flux}\mathcal{N}_{\rm clump}$. As a result, the electron drag force, vortex acting force, and the buoyancy force on a clump are given by

$$f_{\rm drag,coll} \approx \mathcal{N}_{\rm clump}^{3/2} f_{\rm drag} \ , \tag{46a}$$

$$f_{\rm Mag,coll} \approx \mathcal{N}_{\rm clump} f_{f,\rm Mag} \ , \tag{46b}$$

and

$$f_{\rm buoy,coll} \approx \mathcal{N}_{\rm clump}\gamma f_{\rm buoy} \tag{46c}$$

respectively. So the electron drag force becomes dominant when clumping of flux lines is serious or when the quark superconductivity is extremely type I. And from now on, the symbol $\mathcal{N}_{\rm flux}$ should be interpreted as the product of the number of flux quantum in each flux tube and the number of flux tubes in a clump.

Let us consider a $1.4M_\odot$ strange star with (core) radius 11 km whose density in the outer region of the strange core is around 5×10^{14} gm cm^{-3}. The moment of inertia of the star is about 1.6×10^{45} gm cm^2 (Benvenuto et al. 1991b). We also fix $\theta = 45°$. We take a typical star with initial magnetic field $B_{\rm star}(0) = 10^{12}$ G, initial angular speed $\Omega(0) = 2000$ rad s^{-1} (and hence an initial period of about 3 ms), $\gamma = 0.5$, and $\mathcal{N}_{\rm flux} = 1$ as our "reference" star. Then the effects of the initial magnetic field, initial angular speed, the value of γ in the effective buoyancy force, and the number of flux quanta in a flux clump $\mathcal{N}_{\rm flux}$ on the stellar magnetic evolution can be studied by varying these parameters one at a time.

We first investigate the case when there is no clumping, and the system is almost type II. So we set $\mathcal{N}_{\rm flux} = 1$. As shown in Figs. 2a and 3a, both the magnetic field and angular speed remain approximately constant for a while which are followed by power law decays with exponents equal $-1/4$. Their transition times decrease with increasing initial field. In addition, the radial velocities of both the vortices and the fluxoids moves as a whole most of the time (see Fig. 4a).

We can explain both the field and angular speed evolution in a simple way. Since the initial magnetic field is not too high, the star only experiences a modest spin down. Thus, the vortex bundles are effectively pinned to the flux tubes (instead of thermally creep through them) leading to what Ding et al. (1993) called a "co-moving phase". In this phase, $B_{\rm star}(t) \sim \Omega(t)$ and hence the dipole spin down of the star is given by

$$\dot{\Omega} = -\frac{\Omega^3 R_{\rm star}^6 B_{\rm star}^2 \sin^2\theta}{3Ic^3} \approx -\frac{B_{\rm star}^2(0) R_{\rm star}^6 \Omega^5 \sin^2\theta}{2Ic^3\Omega^2(0)} \ . \tag{47}$$

Upon integration, it is easy to show that

$$\Omega(t) \approx \left[\frac{4B_{\rm star}^2(0) R_{\rm star}^6 t \sin^2\theta}{3Ic^3\Omega^2(0)} + \frac{1}{\Omega^4(0)}\right]^{-1/4} \equiv \left[\frac{t}{t_0} + \frac{1}{\Omega^4(0)}\right]^{-1/4} \ . \tag{48}$$

Thus, Ω (and hence $B_{\rm star}$) is almost a constant when $t \ll t_0$ and Ω decays as a power law with an exponent $-1/4$ when $t \gg t_0$. This is consistent with the field and angular speed evolution we have plotted in Figs. 2a and 3a.

Now, we go on to consider the case when clumping is important, and when the quark superconductor is almost type I. We illustrate the situation by putting $\mathcal{N}_{\rm flux} = 10^6$. As shown in Figs. 2b and 3b, when the initial field is low ($\lesssim 3 \times 10^{12}$ G), the magnetic and spin evolution behave almost in same way as in the case when $\mathcal{N}_{\rm flux} = 1$. The huge value of $\mathcal{N}_{\rm flux}$ implies that the electron drag force may be dominant. In order to push the flux tubes, the vortex bundles need to acquire a strong Magnus force by increasing the value of the angular velocity lag ω. Nevertheless, $|\omega|$ cannot exceed its critical value ω_{cr}. So, when the

star spins down too quickly, the vortex bundles in the core have no choice but to thermally creep through the flux tubes leading to what Ding et al. (1993) called the "forward creeping phase". This picture is consistent with the numerical finding that forward creeping phase lengthens with increasing initial magnetic field (see Figs. 4b, c and d). The small radial velocity of the flux tubes at this phase implies that $B_{\rm star}$ remains almost constant. It is until the onset of the co-moving phase due to a much slower spin down rate at later times that $B_{\rm star}$ and Ω decay like $t^{-1/4}$ (see Figs. 2b and 3b).

Now we discuss a more interesting case when $B_{\rm star}(0) = 10^{13}$ G and $\mathcal{N}_{\rm flux} = 10^6$. Fig. 2b shows that $B_{\rm star}$ decays exponentially with a characteristic time of about 5 Myr. However, at about 100 Myr, the decay stays almost constant for a while, and then it decays further like $t^{-1/3}$. Besides, Fig. 3b shows that Ω decreases like a power law with an exponent $-1/2$ for almost 10 Myr. After that, Ω stays almost constant for a while which is then followed by a power law decay with an exponent about $-1/6$.

We can explain the behavior as follows: The rapid spin down due to high value of $B_{\rm star}$ leads to the forward creeping phase (see Fig. 4d). So,

$$\dot{\Omega} \approx -\frac{\Omega^3 R_{\rm star}^6 B_{\rm star}^2(0) \sin^2\theta}{3Ic^3} \tag{49}$$

and hence

$$\Omega(t) \approx \left[\frac{2B_{\rm star}^2(0) R_{\rm star}^6 t \sin^2\theta}{3Ic^3} + \frac{1}{\Omega^2(0)}\right]^{-1/2} . \tag{50}$$

This accounts for the exponential decay in Ω starting from $3Ic^3/2B_{\rm star}^2(0)R_{\rm star}^6\Omega^2(0)\sin^2\theta \approx$ 5 yr. About 10^3 yr or so, the star rotates so slowly that vortex bundle density becomes very low. At this moment, buoyancy becomes the dominant driving force for field decay and hence

$$\dot{B}_{\rm star} = -\frac{2B_{\rm star} v_f}{R_{\rm star}} \approx -\frac{16\gamma E_f(e) c B_{\rm star}}{3\pi^3 e^2 n_e \lambda R_{\rm star}^2 \mathcal{N}_{\rm flux}^{1/2}} \equiv -\frac{B_{\rm star}}{\tau_{\rm buoy}} . \tag{51}$$

That is, $B_{\rm star}$ decays exponentially with a characteristic time $\tau_{\rm buoy}$ of about 4 Myr. Finally at time $\gtrsim 10$ Myr, dipole spin down of the star becomes very ineffective due to the small values of Ω and $B_{\rm star}$. At this time the radial velocity of flux tubes is faster than that of the vortex bundles and the star enters the "reverse creeping" phase (see Fig. 4d and Ding et al. 1993). The pinning force prevents the flux tubes from moving too fast and hence the rate of field decay is decreased. The force balance equation for the flux tubes reads $f_{\rm buoy,coll} - f_{\rm Mag,coll} = f_{\rm drag,coll} \approx 0$ (compare with Eq. (43)). Since $f_{\rm buoy,coll}$ is time independent, $f_{\rm Mag,coll} \propto |\Omega\omega/B_{\rm star}|$, and $\omega \approx -\omega_{cr} \propto |B_{\rm star}|^{1/2}$, the force balance equation implies that $B_{\rm star} \sim \Omega^2$. As a result, $\Omega(t) \sim t^{-1/6}$ and $B_{\rm star}(t) \sim t^{-1/3}$ at the very late stage of the evolution of the star (see Figs. 2b and 3b).

We now turn to the study of the effect of $\Omega(0)$ to the magnetic evolution of the star. Fig. 5 shows that the field decays more rapidly (due to the faster onset of the power law decay) as $\Omega(0)$ increases when the star is in co-moving phase. This agrees with the crossover time estimate given in Eq. (48). However, if the star is in the forward creeping phase, the push received by the flux tubes due to pinned vortices saturates (and thus, independent of Ω). So in this case, the value of $\Omega(0)$ has little effect on the magnetic evolution of the star. I have verified this in some of our runs.

Next, we consider the effect of γ. Again, the only situation where the value of γ can seriously affect the magnetic evolution of a star is when the pinning force is weak at some moment as compared to the buoyancy force; and this happens when both $B_{\rm star}(0)$ and $\mathcal{N}_{\rm flux}$ are large. Fig. 6 show the magnetic field evolution when $B_{\rm star}(0) = 10^{13}$ G and $\mathcal{N}_{\rm flux} = 10^6$. We see that the evolution profile depends quite sensitively on γ. When $\gamma = 0$, we observe the $B_{\rm star} \sim t^{-1/4}$ behavior at late times, indicating that the star is in the co-moving phase. This is reasonable since the only force that push the flux tubes out from the core comes from the vortex bundles. But when $\gamma \gtrsim 0.5$, buoyancy force becomes the dominant. Thus, the magnetic evolution follows an exponential decay when $t \lesssim 10^6$ yr and $B_{\rm star} \sim t^{-1/3}$ at $t \gtrsim 10^9$ yr, indicating that the presence of forward creeping and reverse creeping phase at early and late times respectively.

Finally, we consider the effect of $\mathcal{N}_{\rm flux}$. For $B_{\rm star}(0) = 10^{12}$ G, Fig. 7a tells us that the behavior of the star does not have any visible change $\mathcal{N}_{\rm flux}$ increases from 1 to 10^3. They are all in the co-moving phase. This observation is consistent with the fact that t_0 in Eq. (48) is independent of $\mathcal{N}_{\rm flux}$. It is only when $\mathcal{N}_{\rm flux}$ increases to about 10^6 we begin to see a slow down of field decay due to the presence of a relatively long period of forward creeping phase before the star eventually enters the co-moving phase.

The magnetic evolution is more dramatic if we take 10^{13} G as the initial field. Fig. 7b shows that when $\mathcal{N}_{\rm flux} = 1$, the star is basically in the co-moving phase all the time. When $\mathcal{N}_{\rm flux} = 10^3$, a delay in field decay is observed due to presence of a long period of forward creeping phase at early times. Finally, when $\mathcal{N}_{\rm flux} = 10^6$, the star switches to an initial exponential, followed by an eventual power law delay mode, indicating that the star has locked into the forward creeping $\longrightarrow$ co-moving $\longrightarrow$ reverse creeping pattern.

In summary, we find that in all reasonable parameter range, the value of the initial magnetic field will be reduced to $1/e$ of its original value in less than 1 Myr time when $\mathcal{N}_{\rm flux} \sim 1$ or when $B_{\rm star}(0) \lesssim 10^{12}$ G. If $\mathcal{N}_{\rm flux} \sim 10^6$, the characteristic field decay time is less than 20 Myr provided that $B_{\rm star}(0) \lesssim 3 \times 10^{12}$ G or $\gamma \sim 0$. The only way we obtain a characteristic decay time longer than 20 Myr is by using $\mathcal{N}_{\rm flux}$ as high as 10^6, $B_{\rm star}(0)$ as high as 10^{13} G, and $\gamma \sim 0$ (see Fig. 6) — a set of physically unlikely combination of parameters.

4.6. Observational Implications Of Strange Star Field Decay

The presence of a large number of systematic and random errors in the observed pulsar sample together with the fact that kinematic age sometimes does not truly reflect the real age of a pulsar greatly complicate the analysis of pulsar magnetic field decay. Nonetheless, current statistical analysis and computer simulation of galactic pulsar distribution suggest that the characteristic field decay time is at least 20 Myr (Bhattacharya et al. 1992; Wijers et al. 1993; see also the recent review by Bhattacharya and Srinivasan 1995).

Various authors have studied theoretically the possibility of a magnetic field decay in the core of a neutron star (Sauls 1989; Srinivasan et al. 1990; Chau et al. 1992; Ding et al. 1993). However, Pethick and Sahrling (1995) pointed out recently that the field decay time in the inner crust of a neutron star is at least 80 Myr due to the slow diffusion of the field through the inner crust. Consequently, core magnetic field decay only results in transporting the field from the stellar core to the inner crust; the total stellar field remains unchanged in $\gtrsim 80$ Myr. Therefore, the conventional hypothesis that pulsars are neutron stars is consistent with the observed field decay time of the star.

On the other hand, suggested by our numerical finding in §4.5, the magnetic field of a strange star decays with a characteristic times $\leq$ 20 Myr. In fact, Eq. (51) tells us that the characteristic time for the buoyancy force dominated field decay $\tau_{\rm buoy}$ equals $4.2 \times 10^{-3}\mathcal{N}_{\rm flux}$ Myr. Thus, $\tau_{\rm buoy}$ is longer than 20 Myr only when $\mathcal{N}_{\rm flux} \geq 2 \times 10^7$ — a value which is attainable only when the quark superconductor is extremely type I. Therefore, our finding is inconsistent with the proposition that pulsars are strange stars.

5. Conclusions

In summary, I consider the rotation of a multi-superconducting species object. The rotation of such an object is made possible by the formation of vortices similar to that of superfluid helium. This finding implies the existence of vortex bundles in the core of a rotating superconducting strange star. Because it is energetically favorable for the vortex bundles to pin to magnetic flux tubes, the rotational dynamics and the magnetic field evolution of a strange star are coupled.

Because the nuclear crust of a strange star cannot sustain a strong magnetic stress, the magnetic field evolution of the star is dictated by dynamics of the flux tubes in the core. The core magnetic field evolution due to inter-pinning of magnetic flux tubes and vortex bundles, and clumping of flux tubes is computed numerically. I find that in all reasonable parameter range, the characteristic decay time of the magnetic field is $\leq$ 20 Myr. This finding does not

agree with the hypothesis that pulsars are superconducting strange stars because current pulsar data strongly suggest that pulsar magnetic fields do not decay in 20 Myr.

A number of interesting questions remains. The phase diagram of interacting multiple component superconducting species in rotation remains unclear. It is also interesting to study the effects of alignment torque on magnetic and rotational history of a strange star, and the possible collapse of the nuclear matter crust due to magnetic stress. I plan to report them in my future works.

I would like to thank Mal Ruderman for bringing up this problem to my attention and K. Y. Ding for providing us her field decay program for neutron stars for reference. I would also like to thank H.-K. Lo, Geoff Ravenhall and Frank Wilczek for their useful discussions. The hospitality of Aspen Center for Physics is acknowledged where the early part of this work was performed in the summer of 1995. This work is supported by DOE grant DE-FG02-90ER40542.

A. Solution To The Strongly Interacting Superconducting Species Problem

We prove the following claim by explicitly construct a solution to the problem. For simplicity, we shall drop all the star superscripts over the masses and charges.

Claim: Suppose there is a finite number of superconducting species. Then Eq. (21) has a solution with $K \neq 0$ (and hence it has infinitely many solutions) if and only if there exist two vectors $\mathbf{v}_1 \equiv (M_1, Q_1)$ and $\mathbf{v}_2 \equiv (M_2, Q_2)$ among the (m_j, q_j) together with two rational numbers α_1, α_2 such that $(m_j, q_j) = \beta_{j1}\mathbf{v}_1 + \beta_{j2}\mathbf{v}_2$, with $\{1, \beta_{j1}, \beta_{j2}\}$ being linear dependent over the set of all rational numbers $\mathbb{Q}$ for all j. In addition, $\alpha_1\beta_{j1}+\alpha_2\beta_{j2}$ are rational numbers for all j, and $\alpha_1 Q_2 \neq \alpha_2 Q_1$.

Proof: ($\Rightarrow$) By replacing vectors $\mathbf{v}_i$ by $\mathbf{v}_i/\ell$ ($i = 1, 2$) where ℓ is the least common multiple of the denominators of $\alpha_1\beta_{j1} + \alpha_2\beta_{j2}$, then β_{ji} will be replaced by $\ell\beta_{ji}$. In addition, we can replace α_i by $\lambda\alpha_i$ where λ is the least common multiple of the denominators of α_i and $\alpha_1\beta_{j1}+\alpha_2\beta_{j2}$. Then it is easy to verify that $\lambda\alpha_i$ and $\ell(\alpha_1\beta_{j1}+\alpha_2\beta_{j2})$ are all integers. Thus, we can always assume that α_1, α_2 and $\alpha_1\beta_{j1} + \alpha_2\beta_{j2}$ to be integers instead of rational numbers.

Suppose $\mathbf{v}_1$ and $\mathbf{v}_2$ are linear dependent on each other, then clearly the ratio of m_j to q_j are the same for all j. So, by choosing $N_j = 0$ for all j, $K = 1$, and $\Phi_v = m_j c/q_j$, Eq. (21) is satisfied. Now, we consider the more interesting case when $\mathbf{v}_1$ and $\mathbf{v}_2$ are linear independent

vectors. Consider the equation

$$\begin{pmatrix} P_1 \\ P_2 \end{pmatrix} = \begin{pmatrix} M_1 & -Q_1 \\ M_2 & -Q_2 \end{pmatrix} \begin{pmatrix} K/h \\ \Phi_v/hc \end{pmatrix} . \tag{A1}$$

The linear independence of $\mathbf{v}_1$ and $\mathbf{v}_2$ implies that $M_1Q_2 - M_2Q_1 \neq 0$, and the solution of the above equation is given by

$$\begin{pmatrix} K/h \\ \Phi_v/hc \end{pmatrix} = \frac{1}{M_2Q_1 - M_1Q_2} \begin{pmatrix} Q_1P_2 - Q_2P_1 \\ M_1P_2 - M_2P_1 \end{pmatrix} . \tag{A2}$$

Clearly, by choosing $P_1 = \alpha_1$ and $P_2 = \alpha_2$, we can check that the K given by Eq. (A2) is non-zero.

Now for each j, it is easy to check that by choosing $N_j = \alpha_1\beta_{j1} + \alpha_2\beta_{j2}$ (which is an integer, and this is possible because $\{1, \beta_{j1}, \beta_{j2}\}$ is linear dependent over $\mathbb{Q}$) together with $K(\neq 0)$, Φ_v given in Eq. (A2), then Eq. (21) is satisfied. (Clearly, if N_j, K, Φ_v is a solution of Eq. (21), then so is λN_j, λK, $\lambda\Phi_v$ for any non-zero integer λ. Thus, Eq. (21) has either no solution, or infinitely many solutions.) □

($\Leftarrow$) On the contrary, suppose that for any linear independent vectors $\mathbf{v}_1$ and $\mathbf{v}_2$ chosen among (m_j, q_j), and any rational numbers α_1 and α_2, we can find an j such that $(m_j, q_j) = \beta_{j1}\mathbf{v}_1 + \beta_{j2}\mathbf{v}_2$ with either (1) $\{1, \beta_{j1}, \beta_{j2}\}$ being linear independent over $\mathbb{Q}$; or (2) $\alpha_1\beta_{j1} + \alpha_2\beta_{j2}$ is irrational; or (3) $\alpha_1Q_2 = \alpha_2Q_1$. Now we analyze these three cases one by one:

Case (1): If $\{1, \beta_{j1}, \beta_{j2}\}$ is linear independent over $\mathbb{Q}$, then from Eq. (A1), we know that $N_j = P_1\beta_{j1} + P_2\beta_{j2}$. In order that P_1, P_2 and N_j are all integers, the only possibility is $P_1 = P_2 = N_j = 0$. However, from Eq. (A2), this implies $K = 0$ and hence Eq. (21) has no solution for $K \neq 0$.

Case (2): If $\alpha_1\beta_{j1} + \alpha_2\beta_{j2}$ is irrational, then similar to the argument in case (1), $N_j = \alpha_1\beta_{j1} + \alpha_2\beta_{j2}$ is not an integer. Hence, this choice of α_1 and α_2 does not produce a solution for Eq. (21).

Case (3): If $\alpha_1Q_2 = \alpha_2Q_1$, then $K = 0$ from Eq. (A2), which is impossible. □

The above claim implies that there is, in general, no solution to the strongly interacting limit when the number of different species of superconducting Cooper pairs is greater than or equal to three. On the other hand, solution of Eq. (21) always exists when there are only two species of Cooper pairs, as in the case of strange matter.

REFERENCES

Alcock, C. 1991, in Strange Quark Matter In Physics And Astrophysics, Madsen, J. and Haensel, P., eds., published in Nucl. Phys. B (Proc. Supp.), 24B, 93

Alcock, C., Farhi, E., & Olinto, A. 1986, ApJ, 310, 261

Alpar, M. A. 1987, Phys. Rev. Lett., 58, 2152

Alpar, M. A., Anderson, P. W., Pines, D., & Shaham, J. 1984a, ApJ, 276, 325

Alpar, M. A, Chau, H. F., Cheng, K. S., & Pines, D. 1993, ApJ, 409, 345

Alpar, M. A., Langer, S. A., & Sauls, J. 1984b, ApJ, 282, 533

Andreev, A. F., & Bashkin, E. P. 1976, Sov. Phys. JETP, 42, 164

Bailin, B., & Love, A. 1982, Nucl. Phys. B, 205, 119

Bailin, B., & Love, A. 1984, Phys. Rep., 107, 325

Baym, G. 1988, in Frontiers And Borderlines In Many-Particle Physics, eds. R. A. Broglia, & J. R. Schrieffer (Italian Physical Society, Bologna), 330

Baym, G., Pethick, C. J., & Pines, D. 1969, Nature, 224, 673

Baym, G., & Pethick, C. J. 1975, Ann. Rev. Nucl. Sci., 25, 27

Benvenuto, O. G., & Horvath, J. E. 1989, MNRAS, 241, 43

Benvenuto, O. G., Horvath, J. E., & Vucetich, H. 1991a, Phys. Rev. D, 44, 1321

Benvenuto, O. G., Horvath, J. E., & Vucetich, H. 1991b, Int. J. Mod. Phys. A, 6, 4769

Benvenuto, O. G., & Vucetich, H. 1991, in Strange Quark Matter In Physics And Astrophysics, published in Nucl. Phys. B (Proc. Supp.), Vol 24B, 160

Benvenuto, O. G., Vucetich, H., & Horvath, J. E. 1994, MNRAS, 266, 690

Bhattacharya, D., Van den Heuvel, E. P. J. 1991, Phys. Rep., 203, 1

Bhattacharya, D., Wijers, R. A. M. J., Hartman, J. W., & Verbunt, F. 1992, A&A, 254, 198

Bhattacharya, D., & Srinivasan, G. 1995, in X-Ray Binaries, eds. W. H. G. Lewin, J. van Paradijs, & E. P. J. van den Heuvel (CUP, New York), 495

Cabrera, B. 1987, Japanese J. Appl. Phys. (Supp.), 26, 1961

Chau, H. F., Cheng, K. S., & Ding, K. Y. 1992, ApJ, 399, 213

Ding, K. Y., Cheng, K. S., & Chau, H. F. 1993, ApJ, 408, 167

Farhi, E., & Jaffe, R. L. 1984, Phys. Rev. D, 30, 2379

Haensel, P., Zdunik, J. L., & Schaeffer, R. 1986, A&A, 160, 121

Harvey, J. A., Ruderman, M. A., & Shaham, J. 1986, Phys. Rev. D, 33, 2084

Jones, P. B. 1986, MNRAS, 222, 577

Jones, P. B. 1987, MNRAS, 228, 513

Jones, P. B. 1988, MNRAS, 233, 875

Khalatnikov, I. M. 1957, Sov. Phys. JETP, 5, 542

Leggett, A. J. 1991, in Low Temperature Physics, eds. M. J. R. Hoch, & R. H. Lemmer (Springer-Verlag, New York), 1

Lewin, W. H. G., Van Paradijs, J., & Taam, R. E. 1991, Space Sci. Rev., 62, 223

Link, B., Epstein, R. I., & Van Riper, K. A. 1992, Nature, 359, 616

Madsen, J. and Haensel, P., eds. 1991, Strange Quark Matter In Physics And Astrophysics, published in Nucl. Phys. B (Proc. Supp.), Vol 24B

Mendell, G., & Lindblom, L. 1991, Ann. Phys., 205, 110

Muslimov, A. G., & Tsygan, A. I. 1985, Ap&SS, 115, 41

Page, D. 1992, in Proceedings Of The Workshop On High Energy Phenomenology, eds. M. A. Pérez, & R. Huerta (World Scientific, Singapore), 347

Pethick, C. J., & Sahrling, M. 1995, ApJ, 453, L29

Ruderman, M. 1991a, ApJ, 366, 261

Ruderman, M. 1991b, ApJ, 382, 576

Ruderman, M. 1991c, ApJ, 382, 587

Ruderman, M. 1992, private communications

Sauls, J. A. 1989, in Timing Neutron Stars, eds. H. Ögelman, & E. P. J. van den Heuvel (Kluwer, Dordrecht), 457

Srinivasan, G., Bhattacharya, D., Muslimov, A. G., & Tsygan, A. I. 1990, Current Sci., 59, 31

Vardanyan, G. A., & Sedrakyan, D. M. 1981, Sov. Phys. JETP, 54, 919

Vollhardt, D., & Wölfle, P. 1990, The Superfluid Phases Of Helium 3 (Taylor & Francis, London)

Wijers, R. A. M. J., Verbunt, F., Bhattacharya, D., & Hartman, J. W. 1993, in Isolated Pulsars, eds. K. A. van Riper, R. Epstein, & C. Ho (CUP, New York), 83

Witten, E. 1984, Phys. Rev. D, 30, 272

This preprint was prepared with the AAS LaTeX macros v4.0.

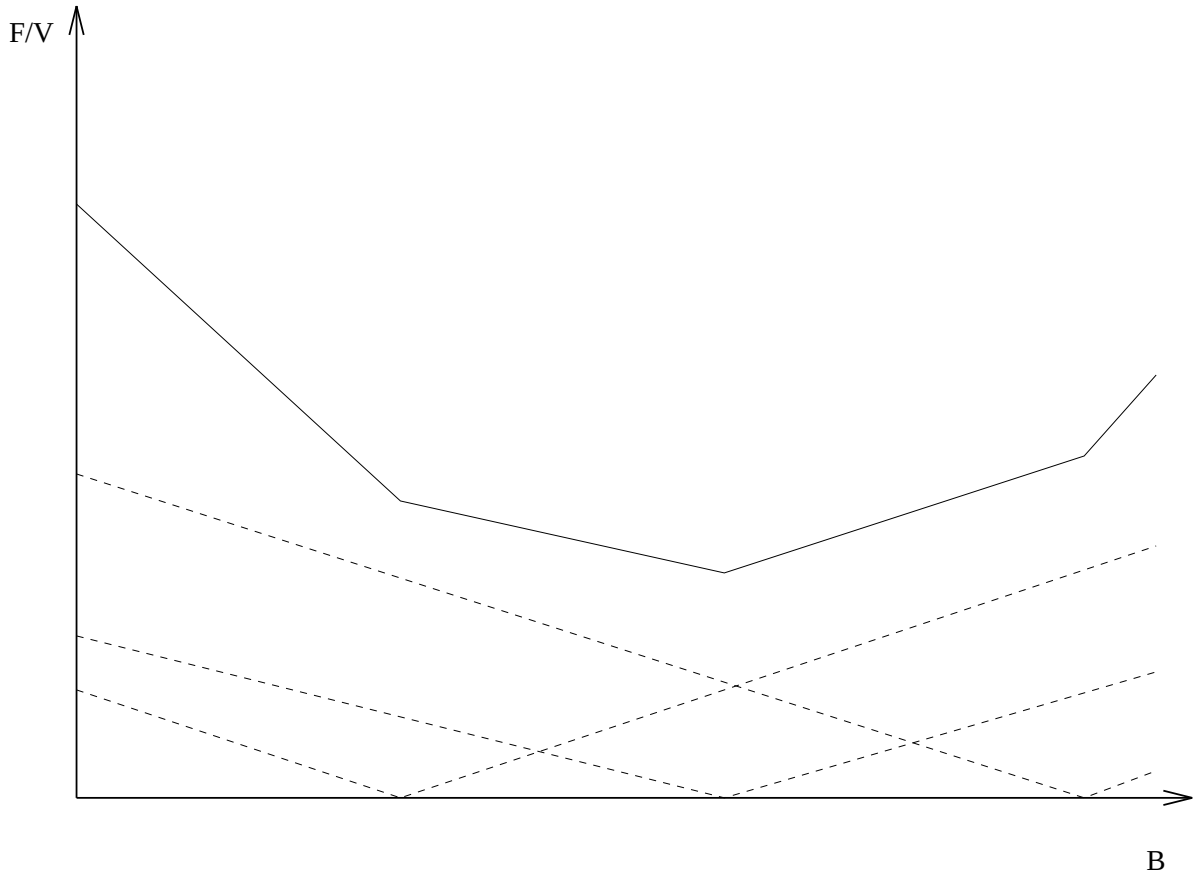

Fig 1

Fig. 1.— Schematic plot of F/V as a function of B for a fixed Ω in a multi-superconducting non-interacting species sample. Dash lines represent the contributions from individual superconducting species, and the solid line is their combined free energy per unit volume.

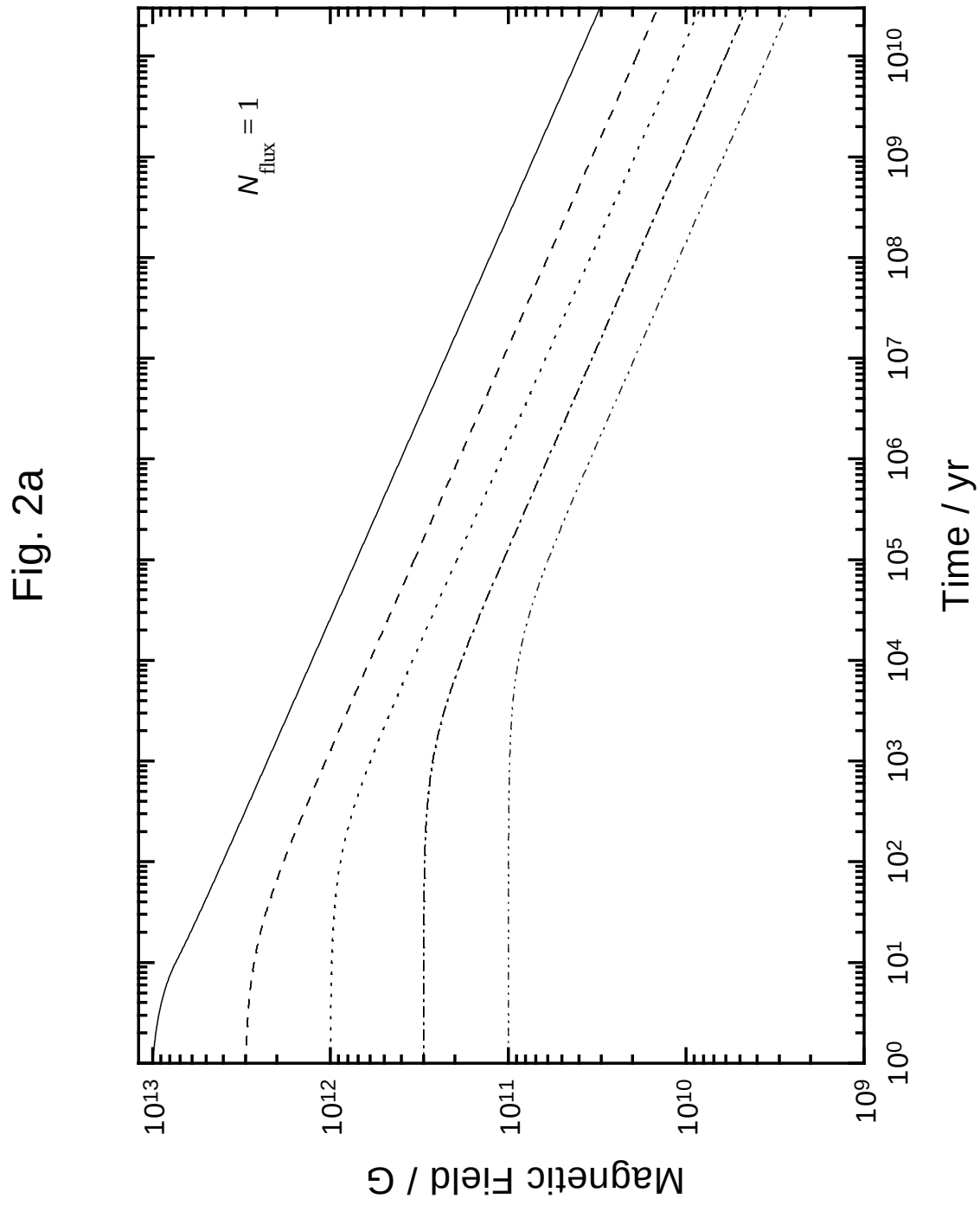

Fig. 2.— The magnetic field decay of a strange star as a function of its initial B field. The initial field measured in G is varied from 10^{13} (solid line), 3×10^{12} (dash line), 10^{12} (dotted line), 3×10^{11} (dash dotted line), to 10^{11} (short dash dotted line). (a) shows the field decay when $\mathcal{N}_{\rm flux} = 1$; while (b) shows the field decay when $\mathcal{N}_{\rm flux} = 10^6$.

Fig. 2b

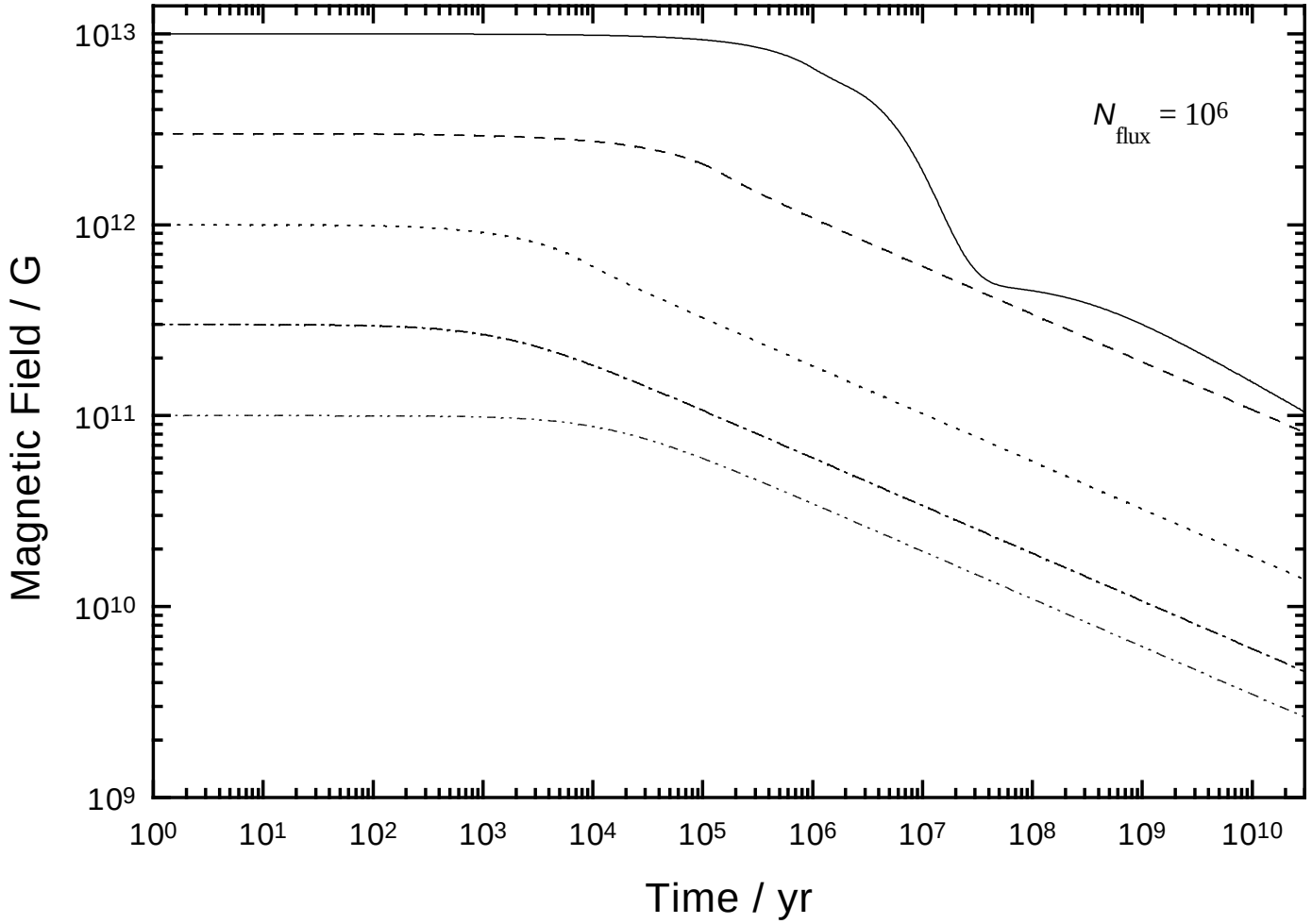
$N_{flux} = 10^6$
Magnetic Field / G
10^{13}
10^{12}
10^{11}
10^{10}
10^{9}
10^0 10^1 10^2 10^3 10^4 10^5 10^6 10^7 10^8 10^9 10^{10}
Time / yr

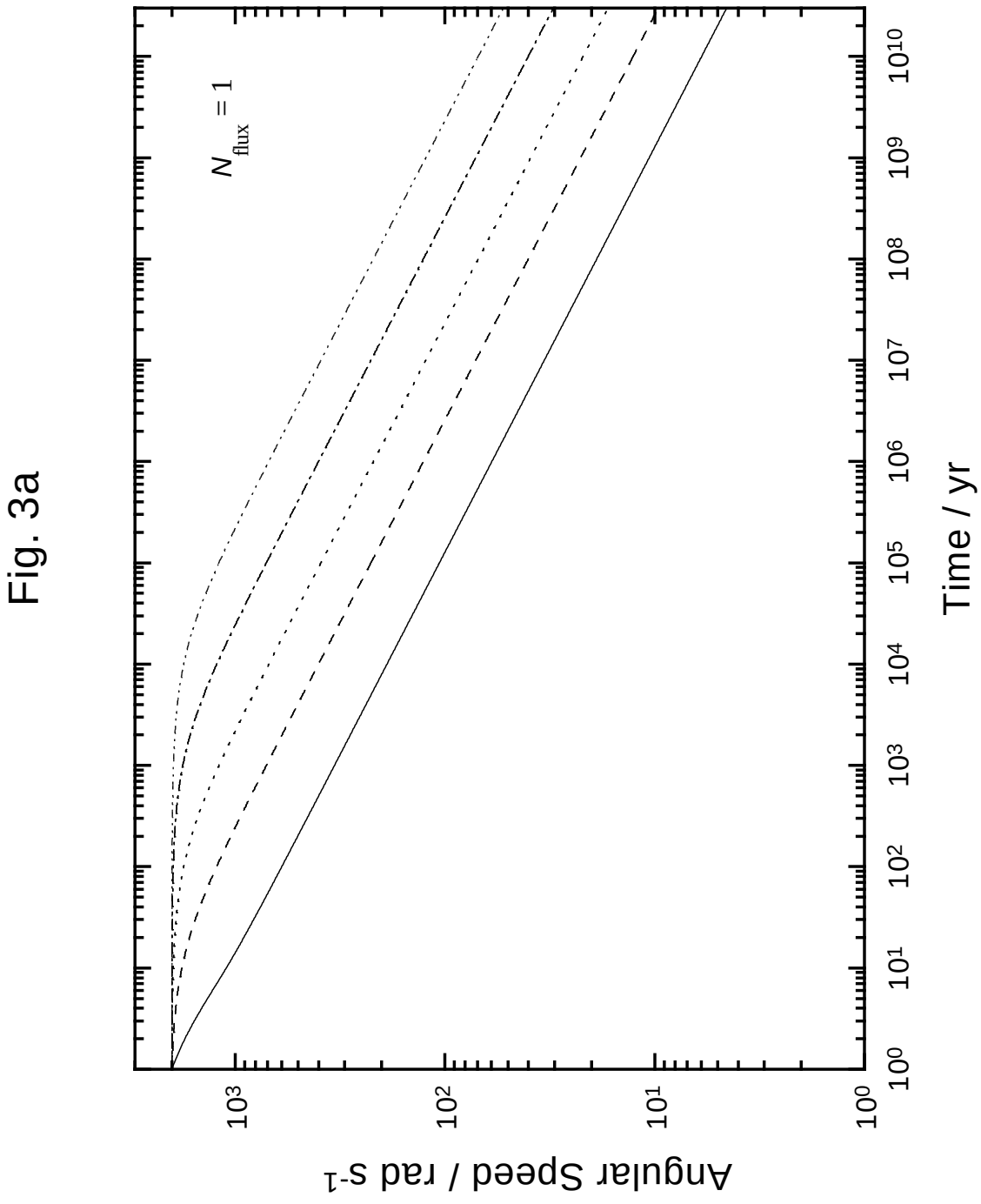

Fig. 3.— Spin down of a strange pulsar as a function of its initial magnetic field. The solid, dotted, dash, dash dotted, and short dash dotted lines correspond to initial magnetic fields of 10^{11}, 3×10^{11}, 10^{12}, 3×10^{12} and 10^{13} G respectively. (a) and (b) are for $\mathcal{N}_{\rm flux} = 1$ and 10^6 respectively.

Fig. 3b

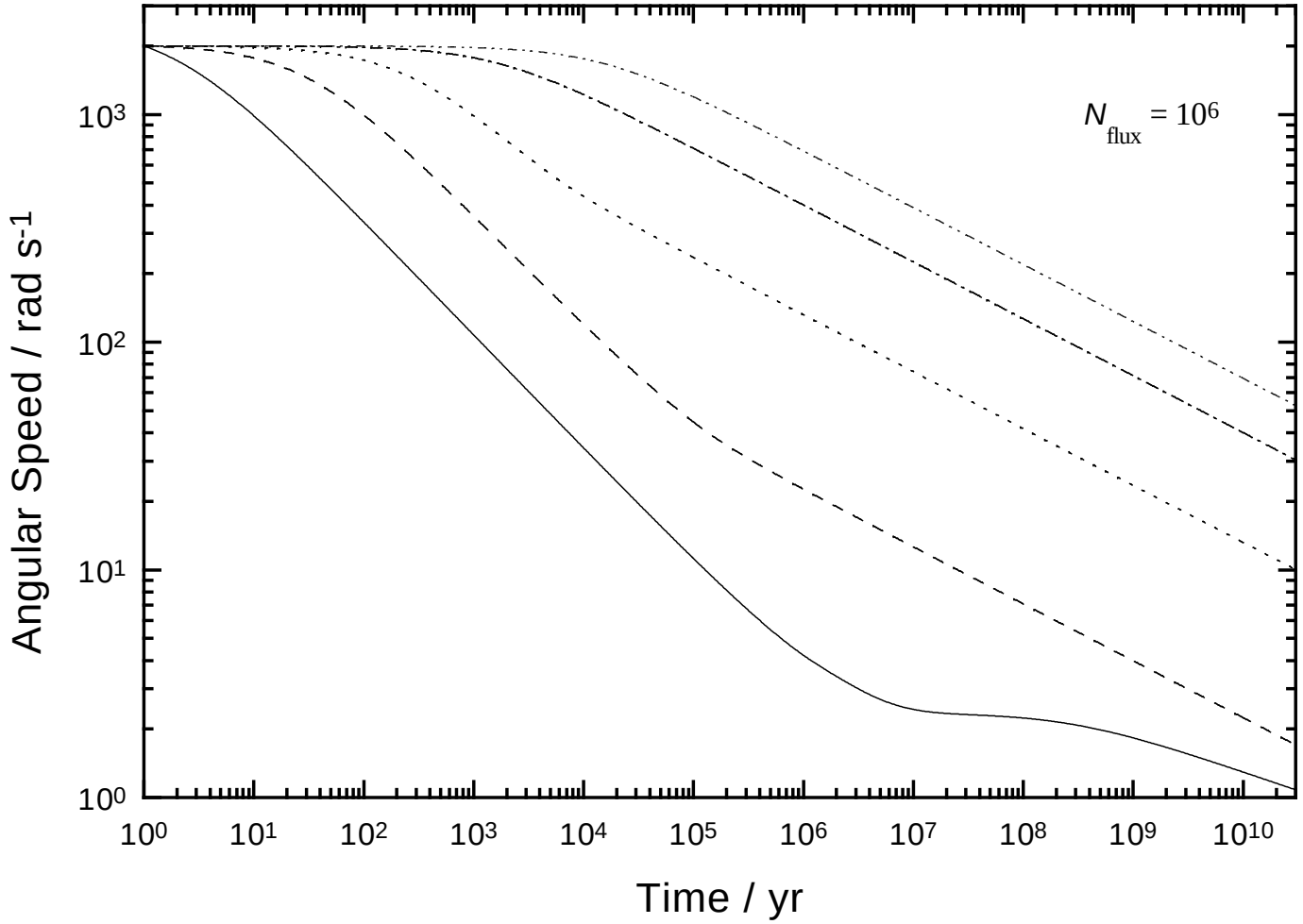
$N_{flux} = 10^6$
Angular Speed / rad s^{-1}
Time / yr
10^0
10^1
10^2
10^3
10^4
10^5
10^6
10^7
10^8
10^9
10^{10}

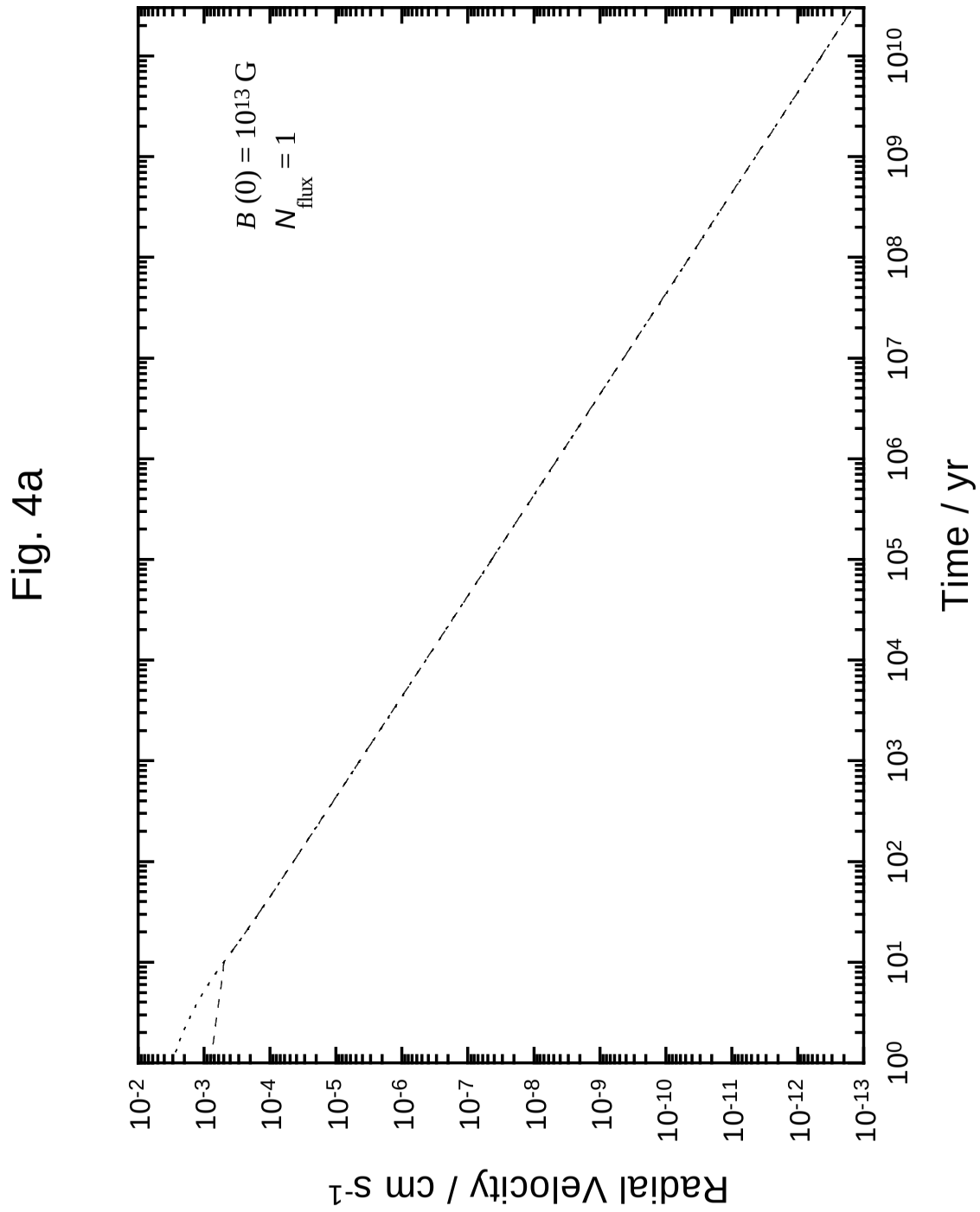

Fig. 4.— Radial velocities of vortex bundles (dotted line) and magnetic flux tubes (dash line) when (a) $B(0) = 10^{13}$ G, $\mathcal{N}_{\rm flux} = 1$; (b) $B(0) = 10^{12}$ G, $\mathcal{N}_{\rm flux} = 10^6$; (c) $B(0) = 3 \times 10^{12}$ G, $\mathcal{N}_{\rm flux} = 10^6$; and (d) $B(0) = 10^{13}$ G, $\mathcal{N}_{\rm flux} = 10^6$. The initial angular velocities in all four cases equal 2000 rad s^{-1}.

Fig. 4b

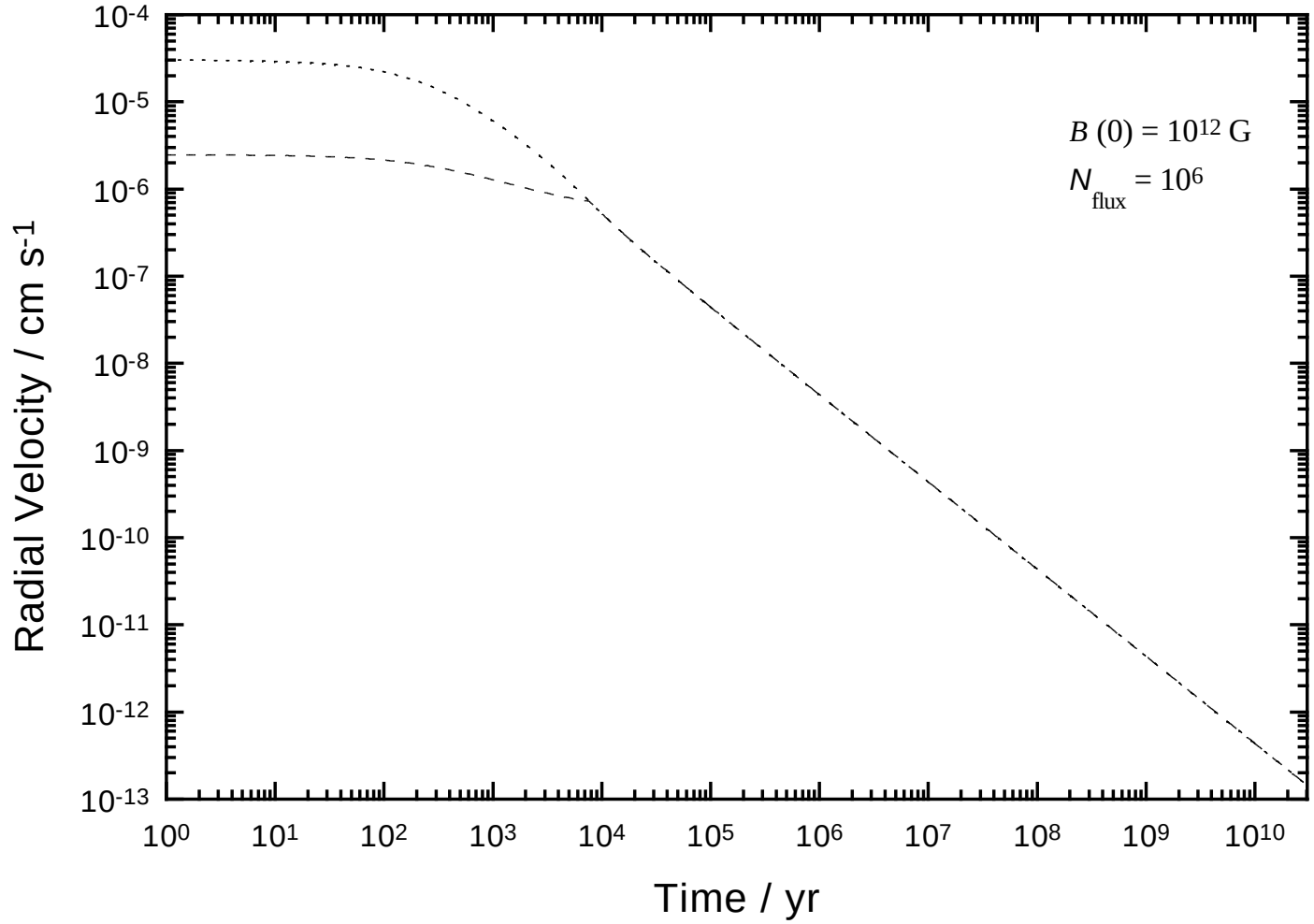
Radial Velocity / cm s-1
Time / yr
B (0) = 10^12 G
N_flux = 10^6
10-4
10-5
10-6
10-7
10-8
10-9
10-10
10-11
10-12
10-13
10^0
10^1
10^2
10^3
10^4
10^5
10^6
10^7
10^8
10^9
10^10

Fig. 4c

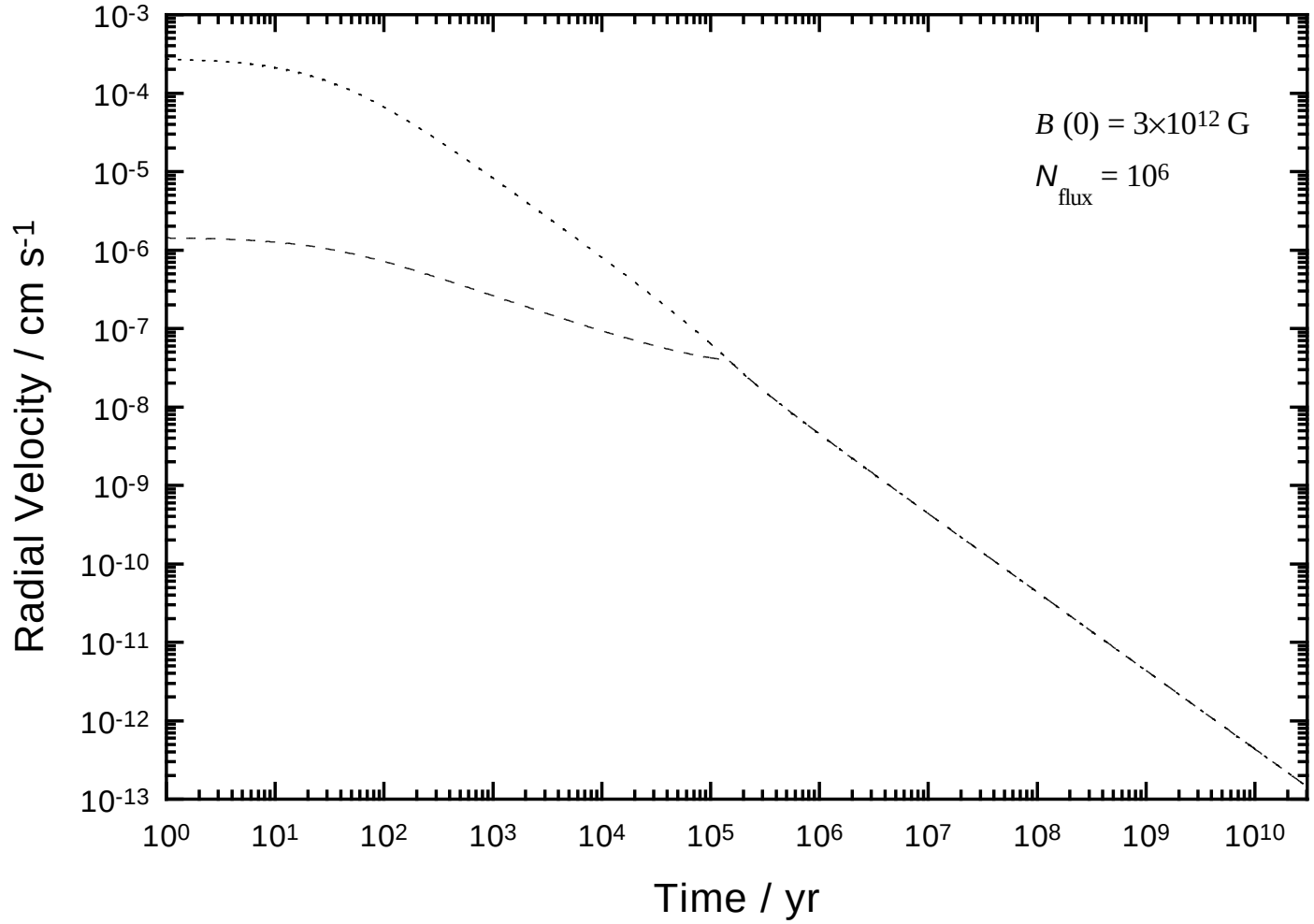
Radial Velocity / cm s-1
Time / yr
B (0) = 3×10^12 G
N_flux = 10^6
10-3
10-4
10-5
10-6
10-7
10-8
10-9
10-10
10-11
10-12
10-13
10^0
10^1
10^2
10^3
10^4
10^5
10^6
10^7
10^8
10^9
10^10

Fig. 4d

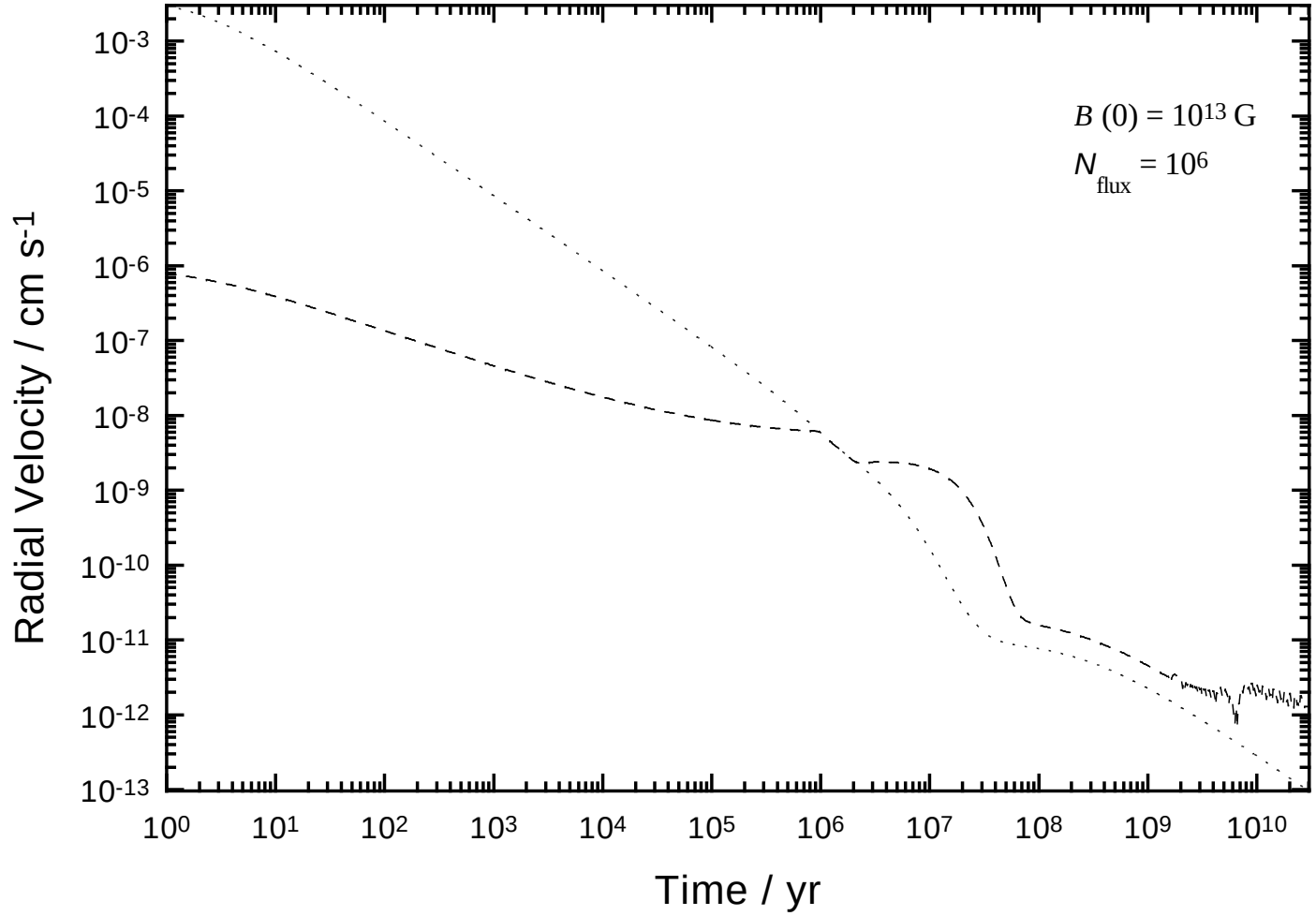
B (0) = 10^{13} G
N_{flux} = 10^{6}
Radial Velocity / cm s^{-1}
Time / yr
10^{-3}
10^{-4}
10^{-5}
10^{-6}
10^{-7}
10^{-8}
10^{-9}
10^{-10}
10^{-11}
10^{-12}
10^{-13}
10^{0}
10^{1}
10^{2}
10^{3}
10^{4}
10^{5}
10^{6}
10^{7}
10^{8}
10^{9}
10^{10}

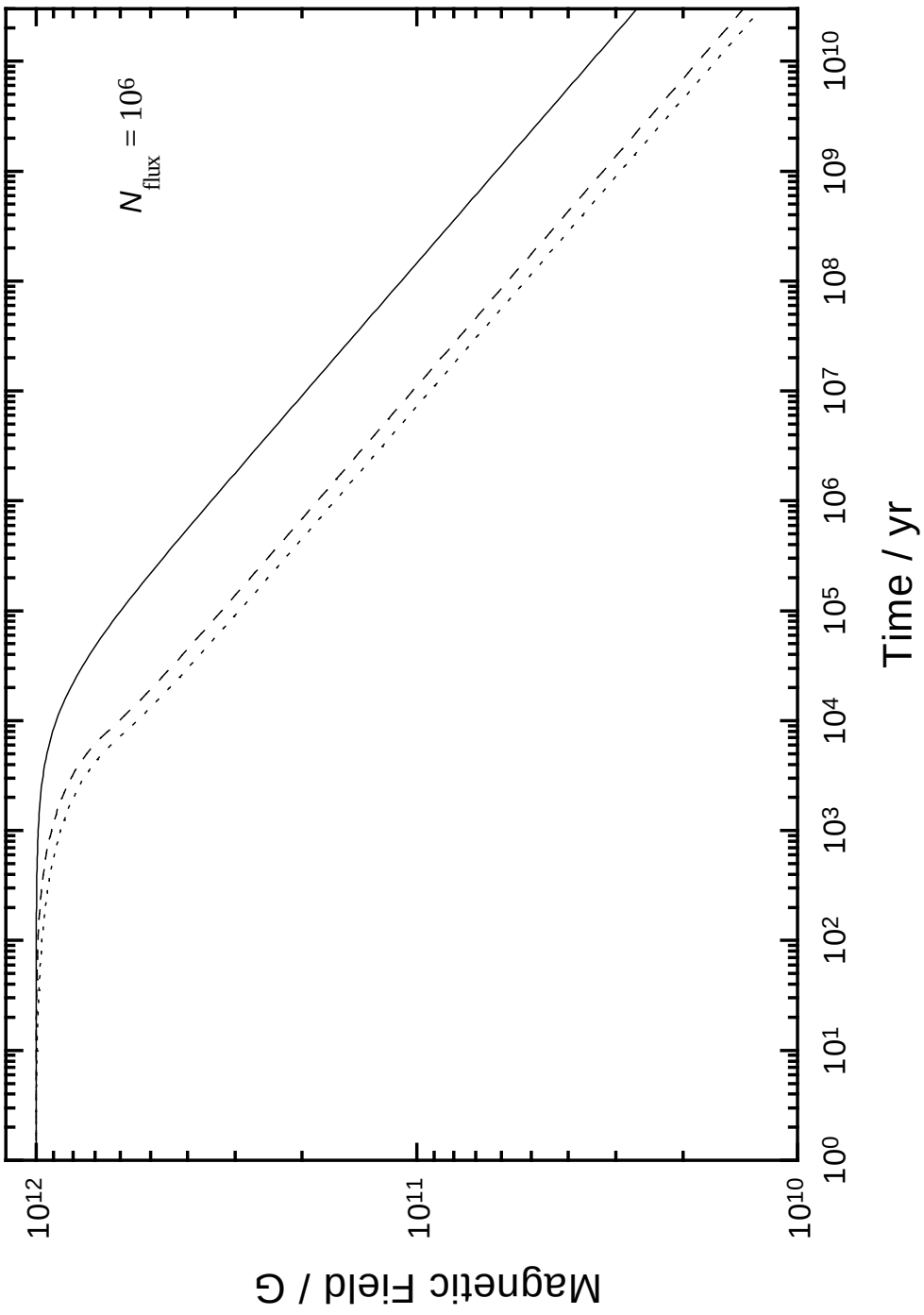

Fig. 5.— Magnetic field evolution as a function of initial angular speed. The solid, dash and dotted lines correspond to initial angular speed of 200, 2000, and 12000 rad s^{-1} respectively. $\mathcal{N}_{\rm flux}$ is set to 10^6.

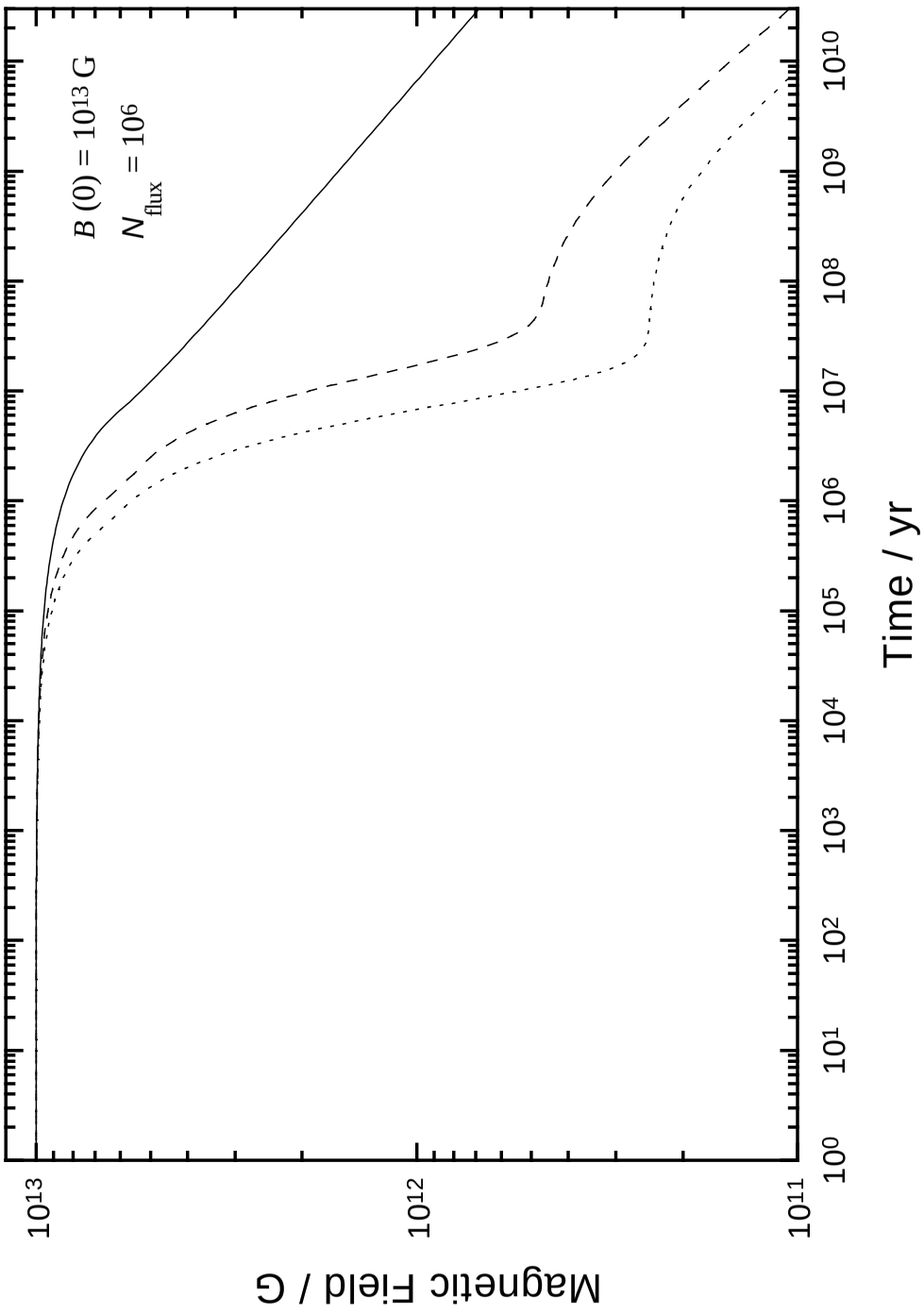

Fig. 6.— Magnetic field evolution as a function of the value γ. The solid, dotted and dash lines correspond to $\gamma = 0$, 0.5, and 1 respectively. Note that the initial magnetic field is set to 10^{13} G.

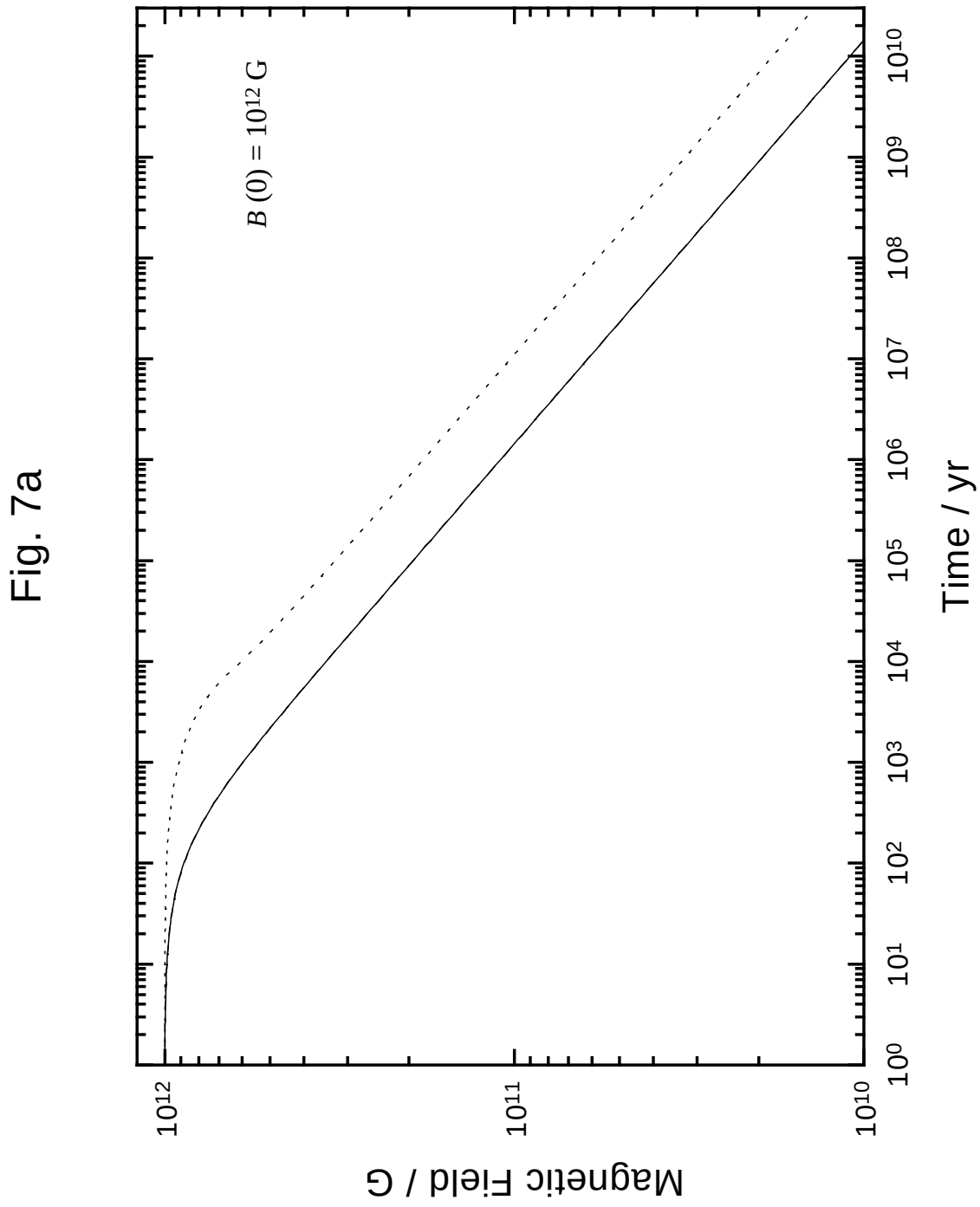

Fig. 7.— Magnetic field evolution as a function of $\mathcal{N}_{\rm flux}$. The solid, dash, and dotted lines correspond to $\mathcal{N}_{\rm flux} = 1$, 10^3 and 10^6 respectively. (a) shows the field decay when $B(0) = 10^{12}$ G, and (b) shows the field decay when $B(0) = 10^{13}$ G. Note that the solid curve overlaps with the dash one in (a).

Fig. 7b

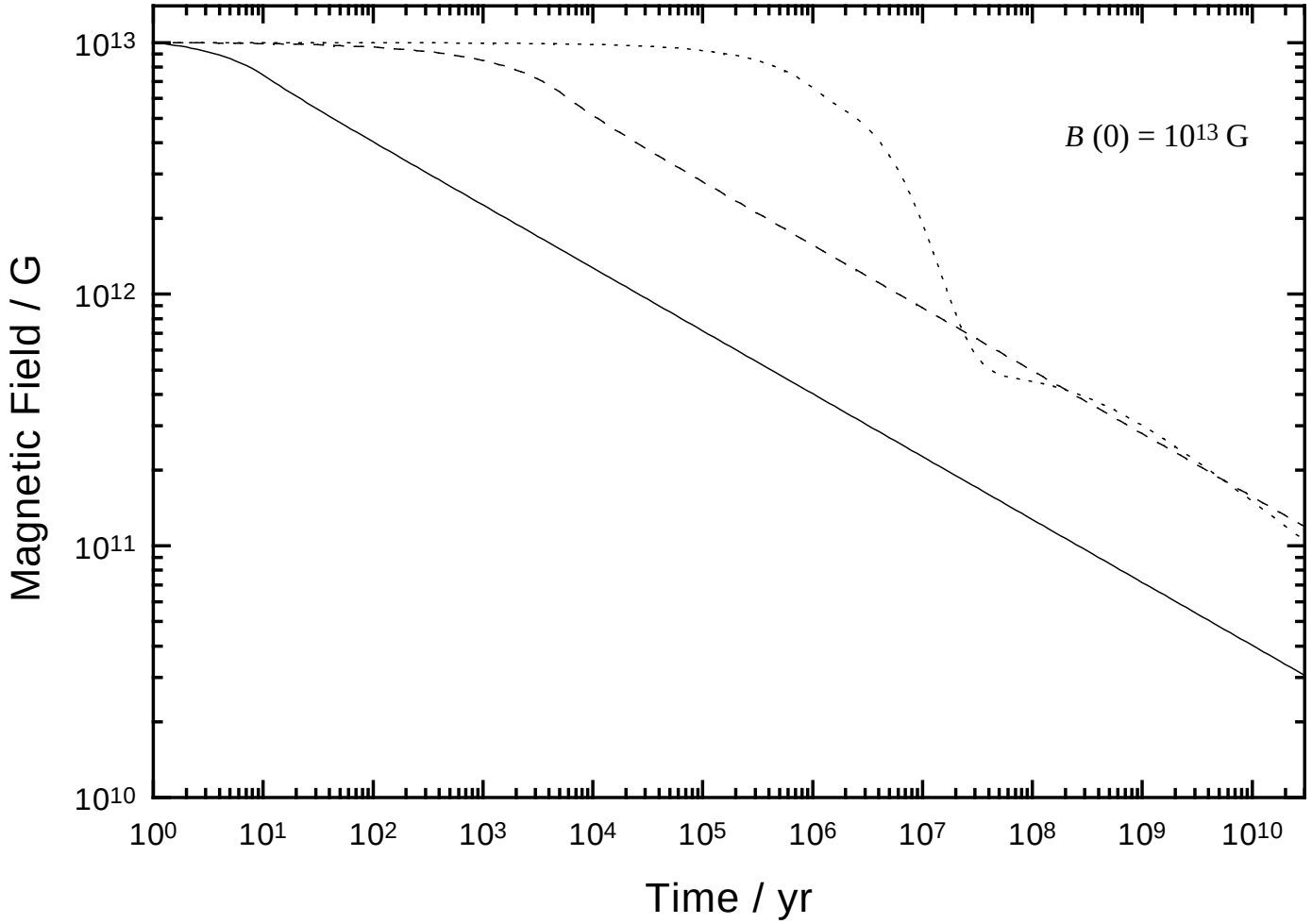
Magnetic Field / G
Time / yr
B (0) = 10^{13} G
10^{13}
10^{12}
10^{11}
10^{10}
10^{0}
10^{1}
10^{2}
10^{3}
10^{4}
10^{5}
10^{6}
10^{7}
10^{8}
10^{9}
10^{10}